UNIVERSITÀ
DEGLI STUDI
DI TRIESTE

UNIVERSITÀ DEGLI STUDI DI TRIESTE

XXXIV CICLO DEL DOTTORATO DI RICERCA IN BIOMEDICINA MOLECOLARE

Dissecting the role of CDK17 in Epithelial Ovarian Cancer

Settore scientifico-disciplinare: BIO/11 BIOLOGIA MOLECOLARE

DOTTORANDO
JAVAD KARIMBAYLI

COORDINATORE
Prof. Germana Meroni

COSUPERVISORE DI TESI
Prof. Guidalberto Manfioletti

SUPERVISORE DI TESI
Dott. Gustavo Baldassarre

ANNO ACCADEMICO 2020/2021

This PhD work was done at Centro di Riferimento Oncologico (CRO, National Cancer Institute) of Aviano, in the Division of Experimental Oncology 2 directed by Dr. Gustavo Baldassare.

Whoever travels without a guide needs two hundred years for a two-day journey.

(Jalaluddin Rumi)

Table of Contents

Abstract i

1.Introduction 1

1.1 Epithelial Ovarian Cancer (EOC) 2

1.1.1 EOC standard treatment 3

1.2 Platinum Resistance 4

1.3 CDKs 8

1.3.1 CDKs as master regulator of cell cycle 8

1.3.2 CDKs and DNA Damage 9

1.3.3 PCTAIREs 9

1.3.4 PCTAIRE Function 11

1.3.4.1 PCTAIREs kinases and their activating partners 12

1.3.4.2 PCTAIREs and Neurobiology 13

1.3.4.3 PCTAIREs and Cancer biology 13

2.Aim of the Study 15

3. Material and Methods 17

3.1 Cell lines 18

3.2 Reagents 18

3.3 Loss-of-function screening 18

3.4 Cell viability assay 19

3.5 Vectors and transfections 19

3.6 Colony Assay 20

3.7 Preparation of cell lysates, Immunoblotting and Immunoprecipitation 20

3.8 Mass spectrometry-based proteomic analyses 21

3.9 Protein stability 23

3.10 Immunofluorescence 23

3.11 EGFR internalization assay and EGF stimulation 23

3.12 In vitro Kinase Assay 24

3.13 Bioinformatic analyses 24

3.14 Statistical analyses 25

4. Results 26

4.1 CDK17 modulation sensitizes EOC cells to PT 27

4.2 CDK17 silencing increases DNA-damage in EOC cells 30

4.3 Identification of CDK17 interactome 32

4.4 CDK17 is involved in EGFR-uptake and internalization mechanisms 38

4.5 CDK17 silencing reduces vesicle loading of EGFR 40

4.6 CDK17 is involved in the sustainment of EGFR signalling 42

4.7 CDK17 is involved in non-canonical phosphorylation of EGFR under CDDP exposure ... 44

4.8 CDK17 promotes AP2A2-EPS15 interaction under CDDP treatment 47

4.9 CDK17 is kinase active and, potentially, is different from canonical CDKs 48

4.10 CDK17 silencing sensitizes EOC cell lines to EGFR blockage 51

5. Discussion 53

6. References 58

7. Publications 66

8. Acknowledgements 68

Abstract

High Grade Epithelial Ovarian Cancers (HGEOCs) is a heterogeneous group of tumours. Late diagnosis and drug-resistant recurrences make HGEOCs the most lethal gynaecological malignancy. The central role played by Cyclin-Dependent Kinases (CDKs), in a plethora of cellular mechanisms, such as control of cell cycle progression, DNA repair, transcription, and apoptosis, make them promising targets to overcome drug-resistance in HGEOCs.

In this thesis we focused on the possible role of CDK17 in the response to platinum (PT) starting from an unbiased loss of function shRNA screening, suggesting that it might play a role in this context. We confirmed by specific targeting that silencing of CDK17 significantly increased PT-induced cell death, in several EOC cell lines. CDK17 (PCTAIRE2) is a member of the largely unexplored CDKs subfamily PCTAIRE whose interactome was unknown. Unbiased proteomic approach looking at CDK17-interacting proteins coupled with functional enrichment analysis identified endocytosis as the most enriched pathway. Network analysis predicted AP2A2 and EPS15, both belonging to endocytosis pathway, among the top score proteins. A subsequent proteomic study to compare the proteins bound to WT CDK17 with those interacting with the clinically relevant CDK17 R312G mutant, demonstrated that WT and mutant CDK17 had the same affinity for EGFR, whose recycling is governed by the binding to AP2A2 and EPS15. Co-immunoprecipitation experiments on endogenous proteins validated CDK17 interaction with AP2A2, EPS15 and EGFR and demonstrated that CDDP-treatment further promotes these interactions. Abrogation of CDK17 expression interferes with EGFR internalization and is associated with reduced ligand-activation of EGFR signalling. Overexpression of CDK17 WT and especially CDK17 R312G mutant maintained a persistent EGFR active phosphorylation and was accompanied by a higher activation of pro-survival signals. Accordingly, EOC cells expressing the CDK17 mutants were more resistant to PT, compared to control and WT counterpart. Moreover, results obtained in PT resistant EOC cells, suggested that CDK17 might contribute to PT-resistance, since its silencing re-sensitize these cells to PT, EGFR inhibition by Gefitinib and their combination. By kinase assay, we showed that CDK17 active complex is able to phosphorylate at different extents EGFR, EPS15 and a subunit of the AP2 complex. Accordingly, CDK17 silencing, concomitantly to PT-treatment, reduced EGFR phosphorylation levels at Threonine residues, further supporting a direct possible involvement of CDK17 kinase activity in the control of stress-induced EGFR activation.

Overall, we have identified a new and unexpected role for CDK17 in the regulation of EGFR pathway that could influence PT-response and cell survival capabilities, that could have a relevant translational impact since CDK17 could represent an novel actionable target of anti-EGFR therapies and a

therapeutic target alone or in combination, in the context of PT-resistant EOC patients for which effective treatments are still lacking.

1.Introduction

1.1 Epithelial Ovarian Cancer (EOC)

Ovarian cancer (OC) is the 8th most common most cancer in women worldwide and the 5th main cause of cancer death in women within the western world, with 259,400 new instances and 184,800 deaths worldwide yearly.[1,2] Asymptomatic early-stages, late diagnosis and the peculiar way of metastatic dissemination give rise to this high mortality-to-incidence ratio, concomitantly to the frequent appearance of chemoresistance.[3,4]

Depending on cellular types of origin, conforming to the anatomic structures from which they arise, ovarian cancer could be subdivided in 3 major clinical categories: Epithelial Ovarian Carcinoma (EOC), originating from the epithelial cells that engulf the ovaries and the fallopian tubes; sex cord-stromal tumour, springing up from the gonadal stroma that surrounds the ovary and germ cell tumour from the germ cells.[5,6] EOC is considered the most lethal subgroup, representing 90% of malignant ovarian tumours. The international Federation of Gynaecology and Obstetrics (FIGO) proposes a 4-steps staging for EOCs, based on the degree of its dissemination at diagnosis. Stage I cancer is confined to the ovaries only, while in stage II, besides the ovaries, the disease spreads to the pelvis and colonizes tubes and uterus. In stage III the disease disseminates to the abdominal cavity and lymph nodes. Finally, in stage IV distant metastasis are evident.[7]

EOC is highly heterogeneous disease and may be subdivided in four principal histological subtypes: serous (SC), endometrioid (EC), clear cell (CCC) and mucinous (MC) epithelial ovarian cancers. Importantly, different histological subtypes vary in aetiology, morphology, molecular biology, and prognosis. Serous tumours include high-grade (HGSC) and low-grade serous (LGSC) classes and represent the majority of the advanced stage ovarian cancers, followed in frequency by clear cell carcinoma. The third most common histotype is endometrioid cancer that might additionally be divided in high and low grade tumours.[8] Finally, mucinous ovarian cancer is the less common histotype. HGSCs represent the 70% of the total epithelial ovarian cancers, while LGSCs, ECs, MCs and CCCs subtypes account for <5%, 10%, 3% and 10%, respectively.[5–7]

According to their molecular alterations, origin, aggressiveness and invasiveness features, EOCs are also subdivided in two major categories: low-grade type I and high-grade type II (Figure 1.1). Low-grade serous, clear cell, endometrioid, and mucinous tumours belong to type I. Type I EOCs in total account for 10% of ovarian cancer associated death. These neoplasms are thought to arise from endometriosis or borderline serous tumours, are well-differentiated, typically limited to the ovary and

exhibit highly stable genomic profile. Type I EOCs are frequently mutated in PIK3CA, PTEN, ARID1A, ERBB2, KRAS and BRAF genes, are relatively dormant and more frequently diagnosed at an early stage[9–11]

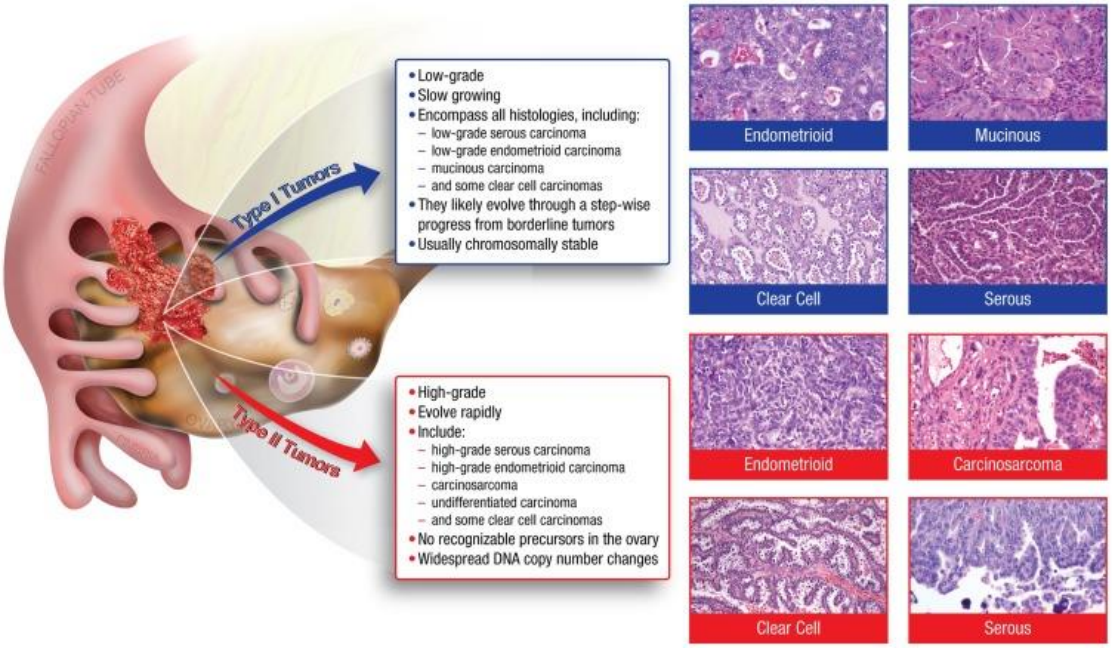

Figure 1.1 Epithelial Ovarian Cancer classification and histopathology. EOCs moleculary and histologically are divided in two categories: Type I tumours (shown in blue) that include low-grade serous, mucinous, endometroid and clear cell carcinomas. In red high-grade serous, endometrioid, clear cell carcinoma and carcinosarcoma are referred to as type II tumours.[12]

Type II EOCs, that include high-grade serous and endometrioid cancers, undifferentiated carcinomas, malignant mixed mesodermal tumours (carcinosarcomas) and some clear cell carcinomas. They mostly originate within the Fallopian tube, display aggressive behaviour, disseminate rapidly, and are diagnosed at later stages. Those tumours exhibit marked genomic instability, significant DNA copy number abnormalities and recurrent mutation in TP53, RB1, BRCA1, BRCA2 and NF1 genes. Furthermore, type II EOCs in nearly half of HGSC cases have been shown to be Homologous Recombination (HR) DNA repair pathway deficient.

1.1.1 EOC standard treatment

The standard first-line treatment for EOCs is based on platinum (PT) drug (cisplatin or carboplatin) in combination with a taxane (paclitaxel or docetaxel) and debulking surgery. Debulking/cytoreductive surgery, which includes hysterectomy, bilateral salpingo-oophorectomy,

tumour debulking and omentectomy, is aimed at eliminating tumour mass to a possible maximum extent, establishing a histopathological diagnosis and FIGO staging.[13]

Paclitaxel is a microtubule-stabilizing agent, that binds to the interior surface of β-microtubule chain and enhances microtubule assembly, by promoting nucleation and elongation phases of microtubule polymerization, that interferes in G2/M cell cycle progression and as a result promotes apoptosis. Consequently, proper mitotic spindle organization is compromised, hence cells cease to successfully complete mitotic division leading to apoptosis.[14] Platinum compounds exert their chemotherapeutic mechanism as DNA-binding alkylating agents and exploit their anti-tumour activity through the formation of intrastrand and interstrand cross-links, interfering with DNA repair mechanisms, causing single-strand (SSBs) and double-strand breaks (DSBs). DSBs require not conservative repair by the error-prone nonhomologous end-joining pathway (G1 phase) or conservative repair through error-free Homologous Recombination (S and G2 phases). Subsequently, this process can induce cell cycle arrest in S and G2 phases, if the damage is limited, or promotes apoptosis in cancer cells, when the DNA damage is extended, mainly through the activation of tumour suppressor p53 pathway[15,16] EOC patients, especially those with high grade EOC, are usually sensitive to first line platinum-based chemotherapy. The response to first line treatment not only divides the patients in chemo-sensitive or -resistant but also is a strong indicator of prognosis and dictates the subsequent lines of therapy. However, more than 75% of sensitive EOC patients develop recurrent, PT-resistant disease.[17]

1.2 Platinum Resistance

Although platinum compounds show a significant degree of efficacy as the first line treatment, relapses are frequent and hinder clinical management and success. Clinically, relapsed EOC patients are categorized into 3 groups according to their follow-up response to platinum treatment, a window between the end of platinum treatment and relapse, referred to as platinum-free interval: 1) platinum refractory (relapses within a month), 2) platinum resistant (relapses within 6 months), 3) platinum sensitive (relapses after 6 months). Such classification is of crucial importance in deciding follow-up treatments (Figure 1.2).[18]

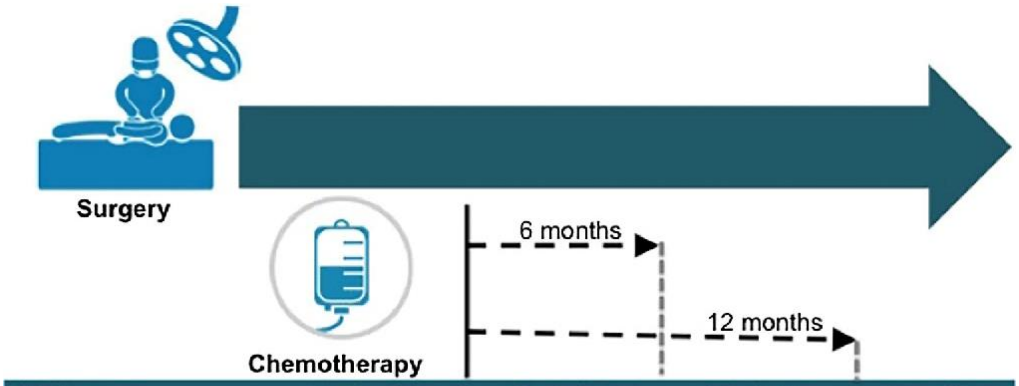

Platinum sensitivity classification	Refractory	Resistant	Partially sensitive	Sensitive
Probability of second platinum response	0%	<10%	30%	>50%

Figure 1.2 Platinum sensitivity classification. Based on the response to platinum chemotherapy patients are classified as refractory, resistant, partially sensitive, or sensitive, according to the time elapsed between the end of first-line treatment and the relapse. Probability of second PT response is shown.[19]

Schematically, PT-resistance could also be divided into two categories: 1) intrinsic and 2) acquired. EOC is characterized by an extensive intra-tumoral heterogeneity composed of multiple, genetically distinct clones. In acquired resistance, a small portion of PT-resistant HGEOC cells exist before treatment and emerges only when the PT-sensitive counterpart is eliminated by treatment.[20] This "clonal selection" results in the repopulation of the tumour and low probability that it will respond to subsequent PT-treatments. This pre-existing resistance could also justify the high rates of relapses and the high percentages of PT-refractory phenotype. Intrinsic PT-resistance is quite infrequent in EOC patients, while acquired PT resistance is very common and has been linked to the alteration of several processes. Despite the initial sensitivity to chemotherapy, small populations of cells tend to adapt preventing cell death with the repopulation of the tumor bulk, leading to rapid relapse and resistance. Therefore, there is an urgent need for a comprehensive understanding of the underlying mechanisms and molecular alterations that could explain disease occurrence and of the same importance, recurrence and resistance, and ultimately, translating that knowledge into alternative therapeutic regimens. Genomic studies showed that HGSOC presents widespread copy number alterations (CNAs) that lead to a very complex genomic landscape. One of the most frequently amplified genomic loci, observed in more than 20% of cases, include cyclin E1 (CCNE1) and MYC genes, as early events that confer PT-resistance in EOC. The amplification and subsequent overexpression of CCNE1 have been reported as one of the major molecular mechanisms that promote the progression of HGSOC. On the other side HGSOC are characterized overall by a low tumour point mutation burden; the most commonly mutated gene is TP53 in the 96% of cases in The

Cancer Genome Atlas (TCGA). Notably, mutations in commonly mutated oncogenes as KRAS, BRAF, NRAS and PIK3CA are very rare (less than 1% in TCGA). However, in this complex scenario, a signature of HR deficiency (HRD) is observed in about half of HGSOC, due to genetic or epigenetic alterations in its key components.[10] Indeed, germline and somatic mutations in BRCA1 and BRCA2 genes are present in 22,6% and 6-7% of high-grade serous EOCs, respectively. In addition to mutations, BRCA1 can be inactivated via promoter hyper-methylation, which is mutually exclusive with respect to BRCA1/2 mutations and is recorded approximately in 10-20% of EOCs (defined as "BRCAness phenotype.[21] As HR being one of the major DNA repair pathways involved in repairing DNA lesions induced by PT-based compounds, therapeutic opportunities may arise in targeting vulnerabilities originating from the defective HR repair machinery. Accordingly, HGEOC patients carrying BRCA1/2 mutations are particularly sensitive to platinum and usually displays a better prognosis. Accumulating clinical evidences demonstrated that these patients can benefit of specific targeted therapies, specifically PARP (poly-ADP-polymerase) inhibitors (Olaparib, Niraparib and Rucaparib), used alone or in combination with platinum, exhibiting synthetic lethal effects when applied to cells with defective HR repair pathway.[22] PARP inhibitors have been approved for the treatment of recurrent ovarian cancer after response to chemotherapy or for germline BRCA-mutated ovarian cancers after chemotherapy progression. Niraparib is also indicated as maintenance therapy after response to first-line platinum-based chemotherapy. However, the restoration of HR repair systems, by reversion of BRCA mutations or intragenic deletions in BRCA1 and BRCA2 mutated genes, contribute not only to platinum, but also to PARP-inhibitors acquired resistance development, suggesting coexistence of overlapping resistance mechanisms under therapy pressure.[23] To circumvent resistance, other targeted therapies are being extensively evaluated, based on the principles of addictive effects with other effective drugs in EOC as anti-angiogenic, immune checkpoints inhibitors, cell cycle kinase inhibitors.[24] For example, the anti-VEGF monoclonal antibody Bevacizumab monotherapy showed increased Progression Free Survival both as monotherapy and also, as the first line therapy, together with platinum compounds.

The idea of combining PARP inhibition with immune-checkpoint blockade lends itself to the study that demonstrated inhibition of PARP upregulates the surface expression of Programmed Death Ligand 1 (PD-L1).[25] The phase I/II TOPACIO (NCT02657889) clinical trial showed that Niraparib in combination with Pembrolizumab is well tolerated and achieves higher response rate, especially in BRCA wild type and non-HRD patients, than either agent alone.[26]

Moreover, combining chemotherapy with inhibitors of CDK-cyclin complexes in different kind of solid tumours has been an active area of pre- and clinical investigations for past few decades.[27]

Specifically, a recent review from our group strongly suggests to take into consideration using especially CDK4/6 inhibitors together with chemotherapy, as well as combining it with PARP inhibitors in different kinds of ovarian cancers.[28] As a matter of fact, recent findings highlight that the contribution of CDKs to cancerogenesis and tumor resistance is not only due to the alteration of their cell cycle regulatory activities, but also through the deregulation of their non-canonical ones such as DNA damage response and anti-tumour immunity.[29–31] These aspects added knowledge into CDK4/6 clinical utility and are provocative to expand the research avenue toward studying and targeting non-cell cycle related functions of CDKs, as we will discuss in detail in chapter 1.3.2 and 1.3.4. In conclusion, mechanisms of EOC platinum-resistance has been an intensive area of research and can be broadly ascribed to: (1) failure of DNA damage recognition due to defective repair systems, prominently HR (2) increased detoxification of reactive platinum species by glutathione, (3) increased efflux of platinum complexes by active transport, (4) increased Nucleotide Excision Repair (NER) capacity, (5) loss of tumour suppressor p53, and (6) overexpression of anti-apoptotic genes such as BCL-2, as schematically represented in (Figure1.3).[20,32]

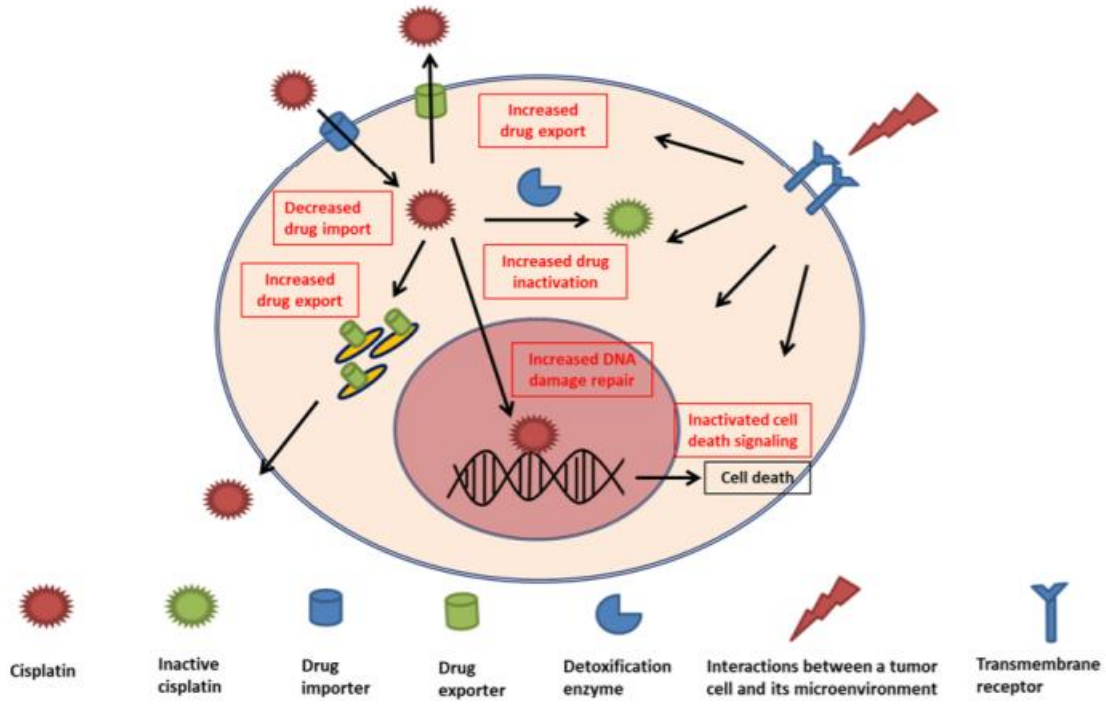

Figure 1.3 Mechanisms of Platinum resistance. A global overview of mechanisms that a cell may employ to overcome PT-mediated cell death, including increased drug efflux, reduced drug uptake, altered drug metabolism, alteration of DNA damage response.[33]

1.3 CDKs

CDKs belong to CMGC family of Serine/Threonine kinases together with Mitogen-Activated Protein Kinases (MAPKs), Glycogen Synthase Kinase-3 beta (GSK3β), members of the Dual-specificity Tyrosine-Regulated Kinase (DYRK) family, and CDK-like kinases.[34] CDKs, as the family name implies, require an activating partner, canonically cyclins, to be functional. Mainly, known as cell cycle master regulators, CDKs bear a multitude of other cyclin-dependent and independent non-cell cycle roles, too.[35] Currently, there are 21 known CDKs, grouped into broadly three phylogenetic subgroups: 1) CDKs involved in the regulation of cell cycle (CDKs 1, 2, 4, and 6), 2) transcription regulatory CDKs (CDKs 7, 8, 9, 12 and 13) and atypical CDKs (CDKs 5, 10, 11, 14–18 and 20) 3) CDKs bearing diverse, yet CDK-specific functions.[36] CDKs are also grouped according to their cyclin binding domain as follow: PSTAIREs (e.g., CDK1), PSSALRE (CDK5), PFTAIREs (CDK14), and PCTAIREs (CDK16), as summarized in Table 1.

Cyclin Binding Domain			
PSTAIRE	**PCTAIRE**	**PFTAIRE**	**PSSALRE**
CDK1	CDK16	CDK14	CDK5
CDK2	CDK17	CDK15	
CDK3	CDK18		

Table 1 CDKs classification according to their cyclin binding domain. In cyclin binding domain, CDK16-17-18 differ by one amino acid from both canonical CDKs (1-3) and their highest homologues CDK14-15.

1.3.1 CDKs as master regulator of cell cycle

Tumorigenesis is the reflection, together with many other mechanisms, of an uncontrolled proliferative state of the cell that represents the result of the deregulated cell cycle. Progression through cell cycle is regulated by CDK-cyclin complexes.[37] The expression of cyclins fluctuates throughout cell cycle fine-tuning the activity of CDKs in different stage of the cell cycle. In the G1 phase, D type cyclins are transcribed in response to mitogenic signals and bind to CDK4/6 to phosphorylate the tumour suppressor RB proteins and allow E2Fs-dependent transcription. This event allows transcription of cyclin E, which binds to, and activates CDK2 leading to G1 to S transition. At this point the cell is committed to conclude the cell cycle and eventually divide in two daughter cells. Sequentially, CDK2 partners with cyclins E and A2 during S phase to duplicate the DNA and during G2 phase to prepare for the mitotic division (M phase). At the end of G2 phase, cyclin A preferentially activates CDK1 to initiate mitosis; during mitosis, cyclin B1 overcomes cyclin A in partnering with CDK1, to ensure cells commitment through mitosis completing division.[37]

1.3.2 CDKs and DNA Damage

Cells are routinely exposed to several stimuli that lead to DNA damage. Along the evolution cells adopted different systems to repair damaged DNA. In first instance CDKs inhibition, ensured by the DNA damage sensor kinases ATM and ATR is necessary for the block of the cell cycle, in S or G2 phases, necessary for the cells to repair the damages and prevent the division of cells bearing a damaged DNA. Moreover, CDKs directly participate in the regulation of specific DNA repair pathways. For instance, DNA-double strand breaks (DSBs) are repaired by two evolutionarily distinct mechanisms: high-fidelity homologous recombination (HR), that employs the no-damaged strand as template for repairing, and non-homologous end-joining (NHEJ), which directly glues broken ends and therefore is error-prone. Increasing evidence indicate the central role of CDKs, not only as master-regulators of cell cycle control but also as fine-tuned modulators of DNA damage response, coupled to transcriptional regulative activities. In this context cyclin A-CDK1/2 and cyclin B-CDK1 complexes by phosphorylating BRCA2 at Ser3291, inhibit its interaction with RAD51 and consequently on HR, ensuring proper cell cycle under normal conditions. CDK2 was shown to promote HR by imposing its kinase activity on C-terminal binding protein 1 (CtIP1). Once phosphorylated, CtIP1 could bind to BRCA1 and MRE11 in repairing DSBs. Also, CDK5 was shown to be activated under DNA-damaging conditions in primary cerebellar granular neurons, and once activated it phosphorylates ATM at Ser 794, thus triggering ATM-governed DNA-damage response.[38] CDK18, which belongs to PCTAIRE CDKs subfamily, has been documented to play a role in ATR-mediated DNA-damage response, that we will describe in detail in chapter 1.3.4.[39]

1.3.3 PCTAIREs

PCTAIREs are arguably the least studied sub-family of CDKs, composed of roughly 500 amino-acid long proteins. Like other CDKs, PCTAIREs are well evolutionarily conserved and share high sequence homology with other CDKs, specifically to PFTAIREs (CDK14 and 15) (60%), CDK1, CDK2 (52-54%) and CDK5 (58%) (Figure 1.4).

PFTAIRE proteins are the most similar of all the CDKs proteins to PCTAIREs. The PFTAIRE family includes two proteins, CDK14 and CDK15. PFTAIRE are expressed highly in neural tissue and generally knowledge about this sub-group of proteins is scarce.[40] As seen in Figure 1.4 homology between PCTAIRE and PFTAIRE families is largely restricted to their kinase domains.

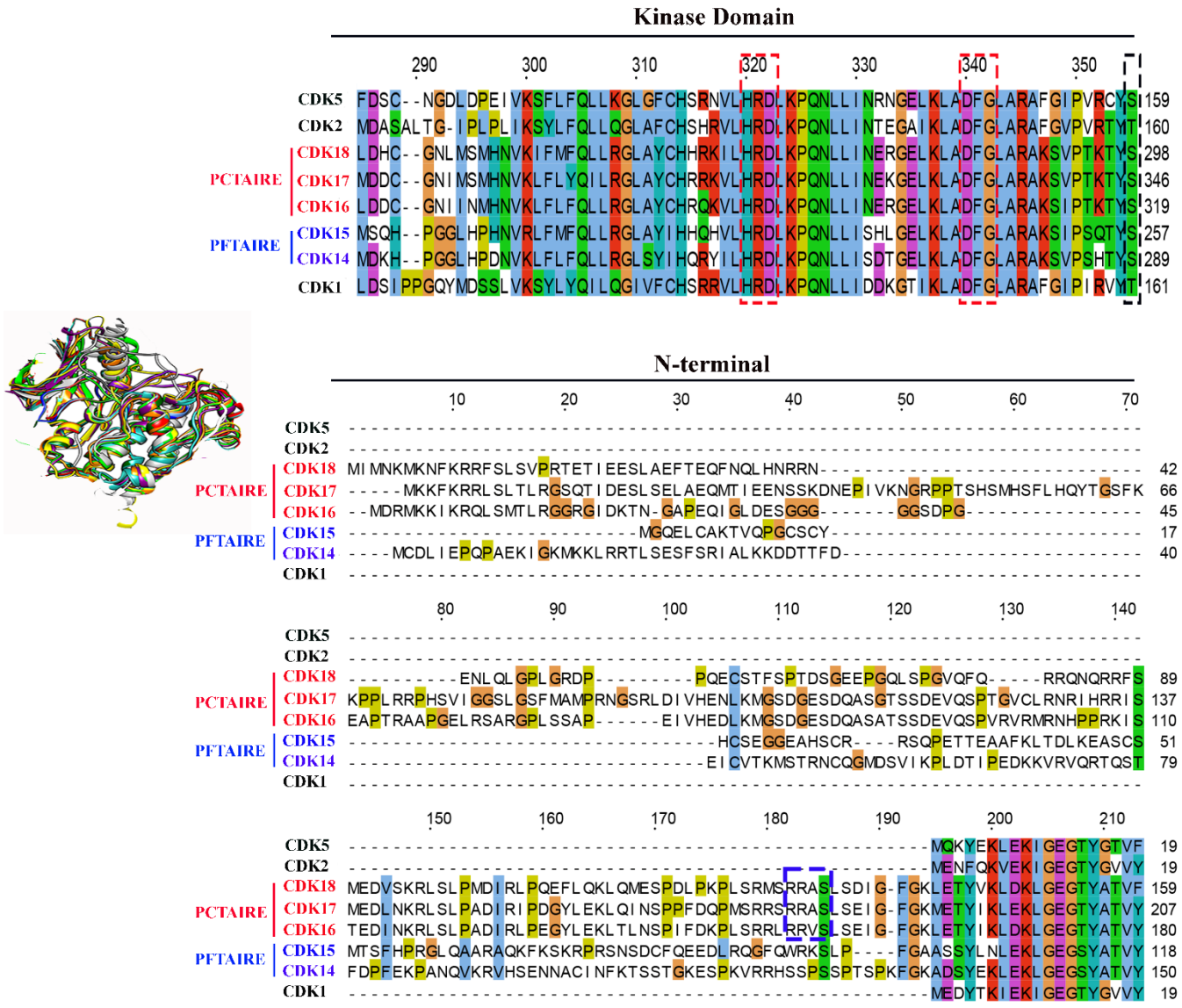

Figure 1.4 Protein sequence similarities of PCTAIREs with other selected CDKs. Protein sequences for CDK1, 2, 5, 14, 15, 16, 17 and 18 were retrieved from UniProt database and aligned in Jalview software. Red frames indicate conserved important motifs included in the kinase domain (defined as HRD and DFG motifs). Black frame indicates conserved Tyrosine residue (161 in CDK1 and 160 in CDK2). Blue frame indicates PLK kinase motif, that was present in PCTAIRE only.

It is well known that cyclin binding triggers structural reconfiguration in CDKs, thus enabling them to exert their kinase activity. By mutagenesis experiments and structural studies, it was shown that pan-kinase conserved motifs like HRD and DFG are indispensable for kinases to become active. As shown in Figure 1.4, (represented in red-dotted frame) those HRD and DFG motifs and their spanning residues are well conserved among all CDKs. Additionally, CDKs have to be phosphorylated by CDK-activating kinases (CDK1 at 161 Threonine residue, CDK2 at 160 Threonine residue) in order

to make the transition from inactive to the active state, complete. Yet, differently from CDK1 and CDK2, P(C/F)TAIREs and CDK5 contain a Serine in place of a Threonine at the corresponding residue, suggesting that similar activation mechanisms also govern these CDKs (Figure 1.4, black-dotted frame). Mutagenesis experiments in CDK2 demonstrated that although mutating 160 Threonine to Serine residue does not diminish its kinase activity, such mutation does impact the fine-tuning activity of CDK2 in cell cycle progression.[41] This could be an important distinction in the regulation of the kinase activity between canonical and non-canonical CDKs. Also different, from canonical cell-cycle CDKs and CDK5, PCTAIRE and PFTAIREs have N and C-termini extensions. However, PCTAIRE and PFTAIRE do not share similarities within their N-terminal extensions (Figure 1.4), suggesting that those extensions might contribute to defining family and protein-specific functions. Finally, it should be noted that even if homology in the N-terminal extension within the PCTAIRE family is weak, we were able to identify, by a domain search, a PKA binding motif (R-R-X-S), which is conserved in PCTAIRE family (Figure 1.4, blue-dotted frame).

Among PCTAIREs, only CDK16 structure is experimentally resolved and Sarah et. al provided comparative analysis with CDK2 and CDK5, highlighting the conservation of sequence level homology also at structural levels.[42] Unfortunately, the CDK16 structure deposited in Protein Databank [PDB id: 5G6V] is missing in N and C termini extensions, preventing the possibility to analyse their contribution to CDK activity and binding to specific substrates.

1.3.4 PCTAIRE Function

PCTAIREs are highly expressed in differentiated tissues like the brain, testis, post-mitotic neurons, and elongated spermatids.[43] When PCTAIRE (CDK16, 17 and 18) was classified as a subgroup of CDK family, early attempts were to find their activating partners, among cyclins with alternate results. More in general, research on PCTAIRE proteins, even if it is in its infancy, in the past two decades was slightly accelerated and led to the definition of their possible roles in different neurobiological processes. More recently, some pieces of evidence suggested that these proteins could also have a relevant role in cancer biology. Based on these notions, we have divided this section into 3 parts: 1) PCTAIREs kinases and their activating partners, 2) PCTAIREs in Neurobiology and 3) PCTAIREs in Cancer Biology.

1.3.4.1 PCTAIREs kinases and their activating partners

CDK16 was the first member of the PCTAIRE family that was shown to have kinase activity toward Myelin Basic Protein (MBP) protein.[43] By two-hybrid assay 14-3-3 proteins were demonstrated to be CDK16 interactors and promoters of CDK16 cyclin driven-kinase activity.[44] Likewise CDK17 was also shown to possess kinase activity toward Histone H1.[45] Although, later study by Hirose, T et.al identified Tudor Repeat Associator with PCTAIRE (Trap) protein as CDK17 partner, this binding did not have impact on CDK17 kinase activity toward Histone H1.[46]

Since the discovery of their kinase activity, it took almost 20 years to identify specific cyclin partners for PCTAIREs. Again the first, evidences come from the study of CDK16 with the demonstration that it interacts with cyclin Y (CCNY) and that this interaction leads to CDK16 localization to the plasma membrane.[47] Mutagenesis experiments on different CDK16 and CCNY constructs, showed that the CDK16 full-length protein is required for proper interaction. Of note, residues 112-121 at N-terminus, included in the kinase domain, and 461-496 C-terminal residues, seem to be crucial for CDK16/CCNY interaction.[47] Accordingly, mutating the Cysteine residue of PCTAIRE into a Serine residue of PSTAIRE (canonical cyclin binding domain of CDK1-3) does not increase the affinity of CDK16 towards CCNY. However, deleting N-terminus diminishes the interaction. Phosphorylation of CDK16 at Ser153 by PKA diminished its binding to CCNY.[47] Shehata et. al showed that CCNY phosphorylation at Ser100 and Ser326 is a prerequisite to drive the binding to CDK16 and kinase activity. Accordingly, bacterially expressed CCNY failed to activate CDK16 in cell-free lysates.[48] More recently it has been proposed that under autophagic stimuli AMPK phosphorylates Ser326 of CCNY, which in turn promotes CCNY-CDK16 interaction and increases CDK16 kinases activity.[49] Another cyclin able to bind to and activate CDK16 is Cyclin Y-like 1 (CCNYL1) as demonstrated by the work of Zheng et al.[50] The authors demonstrated that the binding affinity of CCNYL1 to CDK16, is higher respect to the one of CCNY and also that CDK16-CCNYL1 mutually increases their stability and ultimately, the kinase activity of the complex. [49]

Interestingly, the conditional knockout of CDK16 and CCNYL1 in mice was generated for the first time by Mikolevic et.al, and demonstrated that the CDK16-CCNYL1 complex is essential for terminal differentiation of spermatocytes and the proper spermatogenesis process.[47,50]

While no reports have clearly addressed which is the cyclin binding partner of CDK17, some data suggest that CDK18 interacts with both cyclin A2 and cyclin E2.[51] Yet, its kinase activity toward Rb protein was shown mainly promoted by the binding with Cyclin A2, and further enhanced by PKA-mediated CDK18 phosphorylation[51]

1.3.4.2 PCTAIREs and Neurobiology

CDK16 was shown to regulate neurite outgrowth, validated by the observation that forced targeting of CDK16 into the nucleus abolishes neurite outgrowth.[52] Moreover, the study on the Myocardin Related Transcription Factors (MRTF) knock-out mice showed that CDK16 is a downstream effector of MRTF/Srf, able to regulate cytoskeletal rearrangement and neurite outgrowth through the modulation of CDK5 activity.[53] Other reports also suggest that CDK16 and CDK18 may regulate neurite outgrowth through activating ERK in oligodendrocyte and neuroblastoma cell lines, therefore promoting neuronal differentiation.[54,55]

Interestingly, by two-hybrid screening of an adult human brain library, both CDK16 and CDK18 were found to interact with Sec23Ap protein, which belongs to the COPII complex involved in cargo transport and Endoplasmatic Reticulum (ER) to Golgi transportation.[56] However, the exact mechanism of PCTAIREs action on cargo transport is still unclear. Yet, both CDK16 and Sec23Ap, are known to interact with 14-3-3[44,57] proteins, whose role has been already described in ER-to-Golgi transport.[58] So taken together, it's tempting to speculate that CDK16 and CDK18 are recruited onto the COPII complex by either Sec23Ap or 14-3-3 and/or by both proteins, where these kinases could exert their activity toward transporters and likely also on cargo proteins.

Overexpression of CDK16 in the hippocampal region leads to a significant drop in the learning capacity of otherwise efficient-learning mice.[59] With the help of high throughput techniques, CDK18 expression was found to be upregulated in hippocampal regions upon antidepressant (venlafaxine and fluoxetine) exposure,[60] and in the central nucleus of amygdala region upon alcohol consumption.[61] CDK17 expression is particularly high in terminally differentiated neurons, residing in hippocampal regions and olfactory bulbs.[45] Its expression seems to be further elevated in the Amyloid Precursor Protein (APP) Alzheimer mice model compared to non-transgenic mice. Similarly, CDK18 is overexpressed in Alzheimer's models [62] and both CDK17 and 18 are subject to APP-driven phosphorylation, [63] overall suggesting that PCTAIRE CDKs could have an important role in the pathogenesis of neuronal degeneration.

1.3.4.3 PCTAIREs and Cancer biology

More recent research started investigating the role(s) of PCTAIREs in cancer biology. A role for CDK16 in the stimuli of cancer cell proliferation has been proposed by different authors through diverse mechanisms. These include: CDK16 phosphorylation of TP53 at S315 that trapped TP53 in the cytoplasm and promoted cell proliferation, survival and radioresistance;[64] Phosphorylation of

Protein Regulator of Cytokinesis (PRC1) at Thr481 by CDK16 prevents its nuclear localization, and promotes cell proliferation;[65] Phosphorylation of the cell cycle inhibitor $p27^{kip1}$ at Ser10 that decreased its stability and promoted cell cycle progression. Accordingly, the inactivation of CDK16 rescued $p27^{kip1}$ expression and impaired cell cycle progression.[66,67] Like CDK16, also CDK18 promotes cell cycle progression, where its overexpression causes the accumulation of cells in S and M phases, consequently decreasing the number of cells in G0/G1 phase.[68]

PCTAIREs have also been shown to play a role in cell survival by regulating apoptosis and/or autophagy. In particular, AMPK dependent activation of CCNY-CDK16 promotes autophagy in ULK and Beclin1 dependent-manner.[49] Contrary to CDK16, screening of myristoylated constitutively active kinases suggested that both CDK17 and CDK18 are potential inhibitors of autophagy.[69] Moreover, a role for CDK16 in the regulation of the extrinsic cell death pathway, has been recently observed upon Tumor Necrosis Factor (TNF) stimuli[70].

Of particular interest in ovarian cancer is the proposed a role for CDK18 in the regulation of DNA damage response.[39] Follow-up studies demonstrated that CDK18 silenced cells, when exposed to replicative stress, had more pronounced stalled replication forks, compared to the control group. In this context, CDK18 seemed to regulate the phosphorylation level of RPA (Replication Protein A) proteins.[39] Other reports suggested that CDK18 could interact with the stress signalling proteins, RAD9 and RAD17 contributing to their chromatin localization and henceforth preventing accumulation of DNA damages, by turning ATR-mediated genomic replication stress signalling on.[39,71]

Finally, a role for CDK18 in cytoskeleton regulation and cell adhesion and migration has been described due to its ability to phosphorylate the actin cytoskeleton regulators, cofilin, and MLC.[72]

As noted earlier, CDK17 is the least studied of all PCTAIRE family members, and very few data are reported for this gene in cancer progression and response to therapies. Interestingly, CDK17 seems to be overexpressed in pre and post-menopausal breast cancers [73] and seems to be involved in the regulation of porcine reproductive and respiratory syndrome virus (PRRSV) infection by preventing its internalization into the cells.[74]

CDK17 was also shown to be associated with the development of glioblastoma [75] and with the glycerophospholipid pathway.[76] Moreover, our data obtained using an unbiased loss-of-function screening, suggest that CDK17 could be involved in PT- based chemotherapies response, in EOC cell lines. Overall, these data suggest that CDK17 might play a different role in cancer biology and that it might deserve more specific investigations.

2.Aim of the Study

High Grade Epithelial Ovarian Cancer (HGEOC) is the most lethal disease among the gynaecological malignancies. It is the fourth leading cause of cancer death in women in developed countries. Usually, the disease is diagnosed at late stage, which greatly reduces available therapeutical options. First-line therapy for HGEOCs is optimal surgical debulking followed by combination of platinum-based chemotherapies. However, despite the initial response most patients eventually relapse. Such acquired and/or intrinsic PT-resistance worsens prognosis and urges identifying new actionable targets to improve patients' therapeutic options. Cyclin-Dependent-Kinases (CDK) play pivotal roles in plethora of biological processes such as cell cycle, regulation of DNA damage, regulation of transcription involved in cancer progression and response to therapies but also represent promising actionable targets to explore. We have recently employed a loss-of-function screening targeting all 23 members of CDK family. The screening identified CDK6 and CDK17 as two kinases possibly regulating Platinum induced cell death in HGEOC. The role of CDK6 in HGEOC platinum response has been studied in depth and published by our and other labs. In this PhD project we have explored the role of CDK17 in HGEOC cells response to platinum, identifying novel and unexpected functions of this CDK.

3. Material and Methods

3.1 Cell lines

MDAH-2774 (CRL-10303) (hereafter MDAH), TOV-112D (CRL-11731), OVCAR-8 (NCI 60-0507712), TOV-21G (CRL-11730), COV362 (CRL-1978) cells were from ATCC (American Type Culture Collection); OVSAHO (JCRB-1046) cells were from JCRB Cell Bank (Japanese Collection of Research Bioresources Cell Bank). Platinum resistant OVCAR8 (OVCAR8 Pt-Res) and MDAH (MDAH Pt-Res) cell lines used in this study were previously generated in our laboratory, as described.[77] All these human cell lines were maintained in RPMI-1640 medium (Sigma-Aldrich Co.) supplemented with 10% heat-inactivated FBS, 100 µg/ml penicillin and streptomycin (complete medium) at 37 °C in 5% CO2 atmosphere. Human Epithelial Ovarian cells (HuNoEC, abm#T1074) were purchased from ABM (Applied Biological Materials) and cultured in Pri-grow I medium. The subsequent drug treatment was administrated when the cells reached again a 70-80% of confluence. 293FT cells (Invitrogen Inc.), used for lentivirus production, were grown in DMEM supplemented with 10% heat-inactivated FBS (Sigma-Aldrich Co.).

3.2 Reagents

Carboplatin (CBDCA) and Cisplatin (CDDP) (TEVA Italia), Paclitaxel (TAXOL®, hereafter Taxol) (from ACTAVIS, Dublin, Ireland), Gefitinib (Iressa) (Selleckchem), Cetuximab (Erbitux^{R}, Merck, Italia), Human-EGF (Peprotech), Cycloheximide (CHX) (Sigma Aldrich), MG132 (Calbiochem) were used for the experiments.

3.3 Loss-of-function screening

Lentiviral particles were produced on 96-well plates using 293FT cells transfected using FuGENE HD Transfection Reagent, with the lentiviral based sh-constructs and lentiviral packaging vectors pLP1, pLP2, and pVSV-G (Invitrogen) and pLKO (Sigma) vectors. The sh-CDKs library created was used to perform the loss-of function screening.[30] On day one 1000 MDAH cells/well were seeded in 96-well plates using a robotic liquid handling Hamilton's MICROLAB STARlet. On day two cells were transduced with the specific sh-RNA or the control sh-ctrl. 72 hours post transduction cells were treated with 140 µg/ml (377 µM) of CBDCA (sup-optimal dose respect to the IC50:182.6 µg/mL) for 16 hours. Cell viability was evaluated 24 hours after the end of treatment using CellTiter 96 AQueous cell proliferation assay kit (Promega).

3.4 Cell viability assay

MDAH, OVCAR8, TOV21-G cells were seeded in 96-well culture plates and transduced with Sh-Ctrl and Sh-CDK17 lentivirus. After 72 hours of transduction cells were treated with increasing doses of CDDP for 16 hours and released for 24 hours. Cell viability was evaluated at the end of the treatment using the CellTiter96 AQueous cell proliferation assay kit (Promega). The same schedule of seeding and transduction was applied in MDAH and OVCAR8 cells for 72 hours of Gefitinib treatment. Cell viability was evaluated at the end of the treatment using the CellTiter96 AQueous cell proliferation assay kit (Promega).

In viability assays using CDDP and Gefitinib combined treatment,OVCAR8 Platinum Resistant clone 8 hereafter OVCAR8 Pt Res#8 (clones were generated from a pool of OVCAR8 resistant cells by single cell cloning)[77] Sh-ctrl and Sh-CDK17 cells were seeded in 96- well culture plates, the day after cells were treated for 6 hours with CDDP and then released for 72 hours with Gefitinib. Cell viability was determined at the end of treatments using the CellTiter96 AQueous cell proliferation assay kit (Promega). Absorbance was detected at 492 nm using a microplate reader (Infinite® M1000 Pro, Tecan).

3.5 Vectors and transfections

The CDK17 WT construct (from pDONR223-PCTAIRE, Addgene#23845) was subcloned in the pEGFP-C1 (cloning site EcoRI-BamHI) vector (Clontech). Mutants were generated, previously in our lab, using a QuikChange Site-Directed Mutagenesis Kit (Agilent) and oligonucleotides carrying the indicated mutation.

<u>CDK17 R312G mutagenesis oligos:</u>

FOR 5'-3' CATAGAAGAAAGGTATTGCATGGAGACTTGAAACCACAGAACC

REV 5'-3' GGTTCTGTGGTTTCAAGTCTCCATGCAATACCTTTCTTCTATG

<u>CDK17 K343N mutagenesis oligos:</u>

FOR 5'-3' GAGCCAAGTCAGTTCCCACAAACACCTACTCAAATGAAGTTG

REV 5'-3' CAACTTCATTTGAGTAGGTGTTTGTGGGAACTGACTTGGCTC

pEGFP-C1 vector, pEGFP-CDK17WT, pEGFP-CDK17R312G and pEGFP-CDK17 K343N were transfected in OVCAR8 cells using FuGENE HD Transfection Reagent (Promega) according to the manufacturer's indications. Stable expressing pools were selected by culturing cells with G418 (0.5 mg/ml). For lentiviral production, 293FT cells (Invitrogen) were co-transfected, using a standard calcium phosphate precipitation, with the lentiviral based shRNA constructs (pLKO) and lentiviral vectors pGag-Pol (Sigma) and pVSV-G (Invitrogen). Seventy-two hours after transfection, medium containing viral particles was used to transduce EOC cell lines. pLKO for control (SHC002) and specific shRNAs (shCDK17#1 TRC0000196448, shCDK17#2 TRC0000194654) were purchased from Sigma-Aldrich Co. Stable knock-down clones were selected by culturing cells in puromycin (0.5-1 μg/ml)–containing medium.

3.6 Colony Assay

Cell lines were seeded in 60 mm dishes, in triplicate as follows:

- OVCAR8 cells overexpressing GFP-empty, GFP-CDK17 WT, R312G and K343N constructs:1,000 cells/dish,
- OVCAR8 Pt-Res#8 Sh-ctrl and Sh-CDK17 cells 1,500 cells/dish,
- MDAH Sh-ctrl and Sh-CDK17 cells 2,000 cells/dish.

Cells were treated with CDDP 5 μM for 6 hours and released. Ten days later plates were stained with crystal violet (0.5 mg/ml in 20% Methanol). Plates were then photographed, and colonies were manually counted.

3.7 Preparation of cell lysates, Immunoblotting and Immunoprecipitation

Cell lysates were prepared using cold RIPA lysis buffer (150mM NaCl, 50mM Tris HCl [ph8], 1% Igepal, 0,5% sodium deoxycholate, 0,1% SDS) plus a protease inhibitor cocktail (Complete, Roche),1 mM sodium orthovanadate, and 1 mM dithiothreitol as previously reported.[78] Protein concentrations were determined using the Bio-Rad protein assay (Bio-Rad).

Immunoprecipitations were performed using 700-800 μg of cell lysate in HNTG buffer (20 mM HEPES, 150 mM NaCl, 10% glycerol, 0.1% Triton X-100) plus indicated specific primary antibody and incubating overnight at 4°C. The immunocomplexes were precipitated by protein A or G agarose for 2 hours at 4°C and separated on SDS-PAGE for Western Blot analysis.

GFP-overexpressing cells pull-down experiments were performed according to manufactures protocol, GFP-Trap kit (Chromotek).

For cell fractionation experiments $50x10^6$ cells were seeded, collected and processed according to manufacturer's instructions (Minute™ Plasma Membrane Protein Isolation and Cell Fractionation Kit, Invent Biotechnologies).

For immunoblotting, equal concentrations of protein samples were separated by 4–20% SDS-PAGE (Criterion precast gel; Bio- Rad) and transferred to nitrocellulose membranes (Hybond C; Amersham). Immunoblotting were performed using the following primary antibodies: mouse monoclonal anti-Vinculin (1:1000, Santa Cruz), rabbit monoclonal anti-β-Actin (1:1000, Cell Signaling), rabbit monoclonal anti-EGFR (1:250, Santa Cruz), mouse monoclonal anti-GAPDH (1:1000, Calbiochem-Merck Millipore), rabbit monoclonal anti-EPS15 (1:500, Cell Signaling), mouse monoclonal anti-AP2A2 (1:500, Santa Cruz), rabbit monoclonal anti-pAKT Ser473 (1:1000, Cell Signaling), goat polyclonal anti-total AKT (1:1000, Santa Cruz), rabbit monoclonal anti-CDK17 (1:1000, Santa Cruz), rabbit monoclonal anti-CDK17 (1:500, Bethyl Laboratories), rabbit polyclonal anti-CCNY (1:500, ProteinTech), rabbit monoclonal anti-Cyclin D3 (1:500, Cell Signaling), mouse monoclonal anti- γH2AX(S139) (1:500, Calbiochem-Merck Millipore), rabbit monoclonal antibody anti-pEGFR Y1068 (1:1000, Cell Signaling), rabbit polyclonal anti-pEGFR T669 (Cell Signaling), polyclonal anti-pERK1/2 (1:1500, Cell Signalling), mouse monoclonal anti-total ERK1 (1:1000, Santa Cruz), mouse monoclonal anti-SFPQ (1:1000, Sigma Aldrich), rabbit polyclonal anti-β1-Integrin (GeneTex), mouse monoclonal anti-phospho-Threonine (Sigma Aldrich), mouse monoclonal anti-phospho-Serine (Sigma Aldrich), mouse monoclonal GFP (1:500) (Roche). Antibodies were visualized with appropriate horseradish peroxidase-conjugated secondary antibodies (GE Healthcare), for chemiluminescent detection, with LiteUP Western Blot Chemilumiscent Substrate (Euroclone) or Alexa-conjugated secondary antibodies (Invitrogen) for Odyssey infrared detection (LI-COR Biosciences). Quantification of the immunoblots was performed using the ImageLab software (Bio-Rad), the Odyssey infrared imaging system (LI-COR Biosciences) or the QuantiONE software (Bio-Rad Laboratories).

3.8 Mass spectrometry-based proteomic analyses

Mass Spectrometry analyses were performed at Interdisciplinary Research Institute of Grenoble (IRIG), in collaboration with Dr. Yohann Coutè (**Exploring the Dynamics of Proteomes (www.edyp.fr)**.

Two independent co-immunoprecipitation experiments with GFP-Trap kit (Chromotek) were analyzed according manufactures protocol and analyzed independently. The first one was made up of 3 samples (triplicates of eluates of GFP and GFP-CDK17-WT), and the second one was made of

4 samples (eluates of GFP, GFP-CDK17-WT, GFP-CDK17-K343N, and GFP-CDK17-R312G). The proteins, solubilized in Laemmli buffer, were stacked in the top of a 4-12% NuPAGE gel (Invitrogen). After staining with R-250 Coomassie Blue (Biorad), proteins were digested in-gel using trypsin (modified, sequencing purity, Promega), as previously described.[79] The resulting peptides were analyzed by online nanoliquid chromatography coupled to MS/MS (Ultimate 3000 RSLCnano and Q-Exactive Plus for first experiment, and Q-Exactive HF for second experiment, Thermo Fisher Scientific) using a 140 min gradient. For this purpose, the peptides were sampled on a precolumn (300 µm x 5 mm PepMap C18, Thermo Scientific) and separated in a 75 µm x 250 mm C18 column (Reprosil-Pur 120 C18-AQ, 1.9 µm, Dr. Maisch). The MS and MS/MS data were acquired by Xcalibur (Thermo Fisher Scientific).

Peptides and proteins were identified by Mascot (version 2.7.0.1, Matrix Science) through concomitant searches against the Uniprot database (*Homo sapiens* taxonomy, 20210624 download), a homemade database containing the sequences of the bait proteins, and a homemade database containing the sequences of classical contaminant proteins found in proteomic analyses (bovine albumin, keratins, trypsin, etc.). Trypsin/P was chosen as the enzyme and two missed cleavages were allowed. Precursor and fragment mass error tolerances were set at respectively at 10 and 20 ppm. Peptide modifications allowed during the search were: Carbamidomethyl (C, fixed), Acetyl (Protein N-term, variable) and Oxidation (M, variable). The Proline software[80] was used for the compilation, grouping, and filtering of the results (conservation of rank 1 peptides, peptide length $\geq$ 6 amino acids, false discovery rate of peptide-spectrum-match identifications < 1%,[81] and minimum of one specific peptide per identified protein group). Proline was then used to perform a compilation and grouping of the identified protein groups.

A weighted spectral counts-based comparison of the protein groups identified in the different samples of the first experiment was performed using Proline. For the first experiment, since triplicates were available for each bait, Proline was used to perform a MS1 quantification of the identified protein groups based on razor+specific peptides. Statistical analysis was then performed using the ProStaR software.[82] Proteins identified in the contaminant database, proteins identified with less than two peptides, proteins identified by MS/MS in less than two replicates of one condition, and proteins detected in less than three replicates of one condition were removed. After log2 transformation, abundance values were normalized by median centering, before missing value imputation (slsa algorithm for partially observed values in the condition and DetQuantile algorithm for totally absent values in the condition). Statistical testing was then conducted using limma, whereby differentially expressed proteins were sorted out using a log2(Fold Change) cut-off of 2 and a p-value cut-off of 0.01, leading to FDR of 1.01% according to the Benjamini-Hochberg estimator.

For the second experiment, a weighted spectral counts-based comparison of the protein groups identified in the different samples was performed using Proline. Proteins from the contaminant database were discarded from the final list of identified proteins. To be considered as a potential binding partner of a bait, a protein must be identified only in its eluate with a minimum of 3 specific spectral counts or enriched at least 5 times in its eluates compared to the compared eluate.

3.9 Protein stability

OVCAR8 cells transduced with sh-ctrl or sh-CDK17 were treated with Cycloheximide (CHX, Sigma, 10 µg/mL) or MG132 (10 µM) containing medium for indicated time points. For the stability/stimulation experiments OVCAR8 Sh-ctrl and Sh-CDK17 and OVCAR8 cells overexpressing GFP-empty, GFP-CDK17 WT and R312G constructs were starved, pre-treated with CHX or MG132 and then stimulated with Human Recombinant EGF (Peprotech).

3.10 Immunofluorescence

For immunofluorescence (IF) on cultured cells, cells were plated on coverslips and fixed in PBS 4% paraformaldehyde (PFA) at room temperature, blocked in PBS-1% bovine serum albumin (BSA), and permeabilized in PBS 0.2% Triton X-100. Stains were permeabilized with primary antibodies: pEGFR Y1068(1:300, Cell Signaling), γH2AX (S139) (1:200, Calbiochem-Merck Millipore), EEA1 (1:200, BD-Transduction Laboratories). Then samples were washed in PBS1X and incubated with secondary antibodies (Alexa-Fluor 488- or 568-conjugated anti-mouse or anti-rabbit antibodies, Invitrogen) for 1 hour at room temperature. TO-PRO-3 iodide (Invitrogen) was used to visualize nuclei and Alexa-Fluor 647- Phalloidin (Invitrogen) for F-actin staining. Coverslips were analyzed using the TCS-SP8 Confocal Systems (Leica Microsystems Heidelberg GmbH, Wetzlar, Germany) interfaced with the Leica Confocal Software (LCS) (version 3.5.5.19976, Wetzlar, Germany) or the Leica Application Suite (LAS) software (version 6.1.1, Wetzlar, Germany). At least 8 fields were scored for each cell population and experimental condition. Fluorescence intensity and protein localization were studied using the Volocity® software (PerkinElmer). Quantifications was performed in Fiji software.[83]

3.11 EGFR internalization assay and EGF stimulation

On day one, 700,000 OVCAR8 sh-ctrl and sh-CDK17 cells were seeded on coverslips and following day cells were starved for 5 hours and then incubated on ice for 10 minutes in order to block EGFR on the membrane and block its internalization. Following this pre-incubation, cells were stimulated

with 20 ng/ml of EGF for one hour, in ice. After EGF stimulation cells were washed with PBS1X to remove excess of EGF and then incubated at 37°C to trigger internalization for the following time points: 0, 5, 10, 15 and 20 minutes, in nutrient-deprived media. Collected coverslips were fixed in PFA 4% for IF-staining as described in section 3.10.

For EGF stimulation experiments 700,000 OVCAR8 cells were seeded in 60 mm dishes and then following day cells were starved for 24 hours and then stimulated with EGF at different time points.

3.12 In vitro Kinase Assay

CDK17-CCNY active complex (Signal Chem) and recombinant proteins AP2B1 (OriGene, TP301129), AP2M1 (OriGene, TP301377), EPS15 (OriGene, TP312097), EGFR (OriGene TP710011) were used for *in vitro* kinase assay.

In vitro kinase assays were performed incubating 500 ng of recombinant CDK17-CCNY active complex with 2 µg of EGFR, EPS15, AP2B1, AP2M1 recombinant proteins, for 30 min at 30 °C in the presence of 1.5 µCi of γ32P-ATP (PerkinElmer).

3.13 Bioinformatic analyses

Protein interaction network was constructed by mapping Mass Spectrometry proteomic results into the protein-protein interaction BioGrid, obtained network processed and visualized in Cytsocape software.[84] Identification of the densest hub was done by applying "Molecular Complex Detection" MCODE algorithm, a specific Cytoscape plug-in.[85] MCODE is a graph theoretic clustering algorithm, that detects densely connected regions in large protein-protein interaction networks that may represent molecular complexes.

Mutational status of protein of the interests in EOC cell lines were retrieved from Broad Institute Cancer Cell Line Encyclopaedia (CCLE), https://sites.broadinstitute.org/ccle/,[86] and visualized using Oncoprint function of Complex Heatmap, Bioconductor Package.[87]

For structural analyses, crystal structure of CDK16 [PDB i.d:5G6V], CDK1 without cyclin [PDB i.d: 4YC6], CDK1-CCNB1[PDB i.d: 4YC3] were retrieved from the Protein Data Bank (PDB) and CDK17 structure was generated by homology modelling using CDK16 [PDB i.d: 5G6V] in Modeller software.[88] Structure alignment and visualization was performed using Chimera software.[89]

3.14 Statistical analyses

Statistical significance ($p<0.05$), means, standard deviation, 95% confidence intervals (CIs) were determined by using GraphPad PRISM software (version 6.0) using the most appropriate test, as specified in each figure. Statistical significance was indicated with: * $p < 0.05$, ** $p < 0.01$, *** $p < 0.001$, **** $p < 0.0001$.

4. Results

4.1 CDK17 modulation sensitizes EOC cells to Platinum

Given the importance of CDKs in regulating several biological processes and to evaluate their involvement in PT-sensitivity, our laboratory has previously exploited an sh-RNA loss of function screening, targeting all human 23 CDKs in high-grade EOC cells. We demonstrated that only the silencing of two CDKs, CDK6 and CDK17, significantly increased carboplatin (CBDCA)-induced cell death, respect to control cells (Figure 4.1A) and we have already characterized the role of CDK6 in this context.[30] Here, we have focused our study on the possible role of CDK17 in PT-response.

In order to confirm screening results, we have employed different cell lines representing different histotypes of ovarian cancer: MDAH (Endometroid), TOV21G (Clear Cell Carcinoma) and OVCAR8 (High Grade Serous).

First, we silenced CDK17 expression using two specific sh-RNAs in the same EOC cell line used for the screening MDAH, and treated them with Cisplatin (CDDP), more active than CBDCA in vitro. CDK17 silencing significantly decreased cell survival in MDAH cells and these results were then confirmed in TOV21G and OVCAR8 cells silenced or not for CDK17 (Figure 4.1 B-D). Next, using OVCAR8 cells as High Grade Serous model of EOC, we stably overexpressed the exogenous EGFP-tagged CDK17 wild type (WT) protein showing that it increases CDDP IC50 from 8.8 μM, of control EGFP-expressing cells, to 12 μM (Figure 4.1E), confirming a role for this CDK in the regulation of CDDP-induced death. Interestingly, by analyzing the TCGA High Grade Serous Ovarian Cancer dataset,[10] we found that CDK17 was mutated in 2/500 analyzed cases. Both mutations (specifically R312G and K343N residues) are located in the kinase domain, suggesting that these mutations may have functional or structural consequences. We therefore generated OVCAR8 cell lines stably expressing GFP-CDK17 R312G or K343N and included them in our study. Dose response curve analysis demonstrated that cells expressing the CDK17 mutant proteins are more resistant compared to control cells and to cells expressing WT CDK17, supporting the possibility that CDK17 and eventually these mutations, could be involved in the regulation of response to platinum and/or on the onset of PT-resistance (Figure 4.1E).

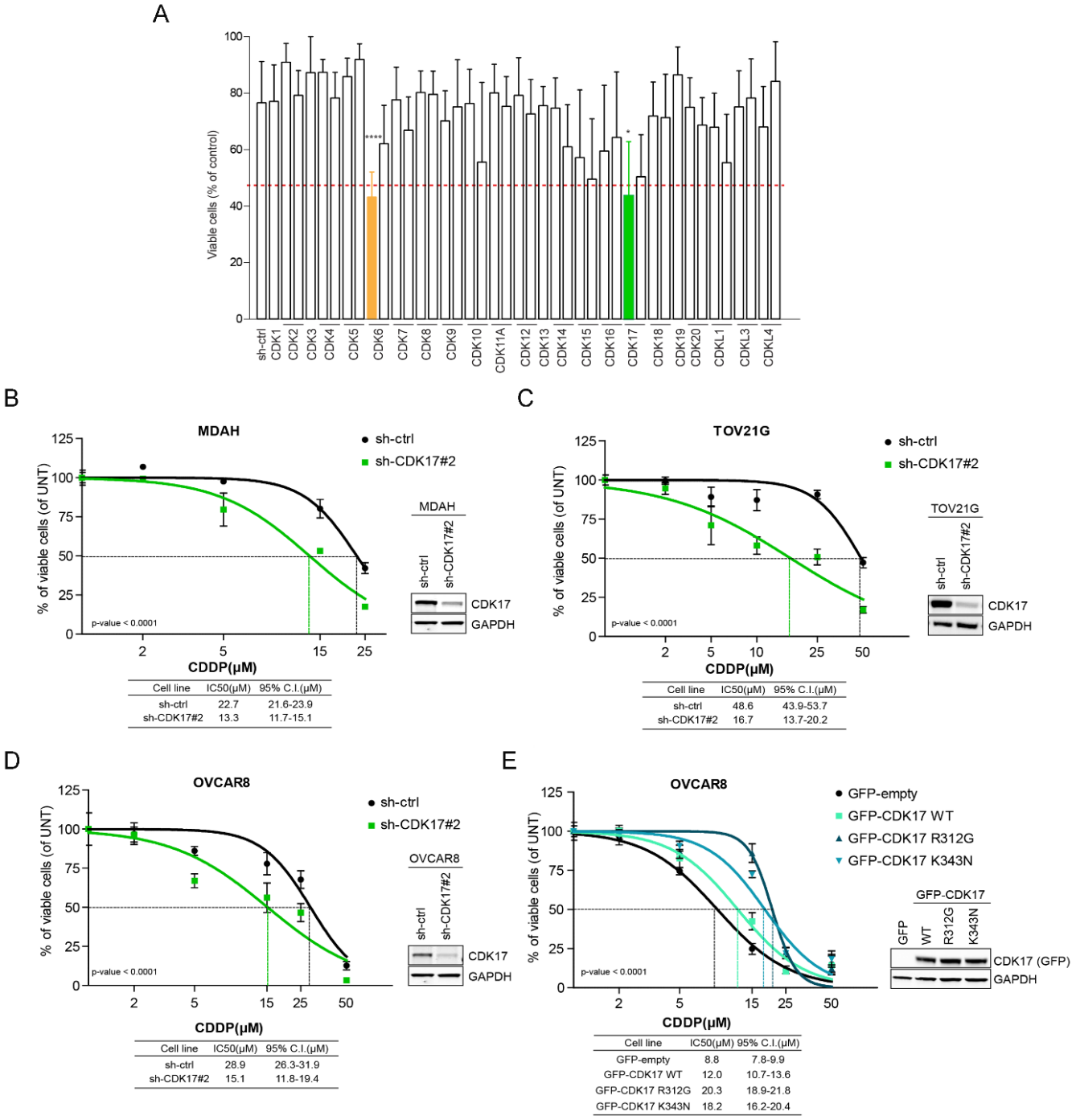

Figure 4.1 CDK17 regulates PT-Response in EOC cells. **A**) Data represent the mean ± SD of 5 independent experiments performed in triplicate and are expressed as survival ratio between CBDCA treated and untreated cells; cells were treated with the sub-optimal dose of 140 μg/ml (377 μM) for 16 hours (MDAH CBDCA IC50:182.6 μg/mL). Red line indicates the pre-specified cut-off of significance (adapted from[30] **B**), **C**), **D**) Nonlinear regression analyses of cell viability in MDAH, TOV21G and OVCAR8 cells, transduced with Sh-ctrl and Sh-CDK17, treated with increasing doses of CDDP for 16 hours and released for 24 hours. The table shows the IC50 and the confidence interval (CI) of each condition. Data are expressed as percentage of viable cells respect to untreated cells and represent the mean (± SD) of 3 biological replicates. Western Blot (hereafter WB) reports the analysis of CDK17 in the same cells transduced with the indicated Sh-RNAs. GAPDH was used as loading control. (**E**) Dose-response curve in OVCAR8 cells, expressing GFP-empty, CDK17 WT, R312G, and K343N constructs, treated with increasing doses of CDDP. Results are expressed as percentage of viable cells respect to untreated cells and represent the mean (±SD) of three independent experiments.

Associated WB displays the expression of respective GFP-tagged constructs. GAPDH was used as loading control. Fisher's exact test was used to calculate the global p-value reported in the graph.

Next, we challenged CDK17 overexpressing OVCAR8 cells in colony formation assays. Cells expressing either WT and/or mutant CDK17 were more resistant to CDDP treatment, if compared to control counterpart (Figure 4.2A-B). In accord with these results, silencing of CDK17 in MDAH cells, as well, significantly reduced their colony formation capacity under CDDP treatment, respect to controls (Figure 4.2 C).

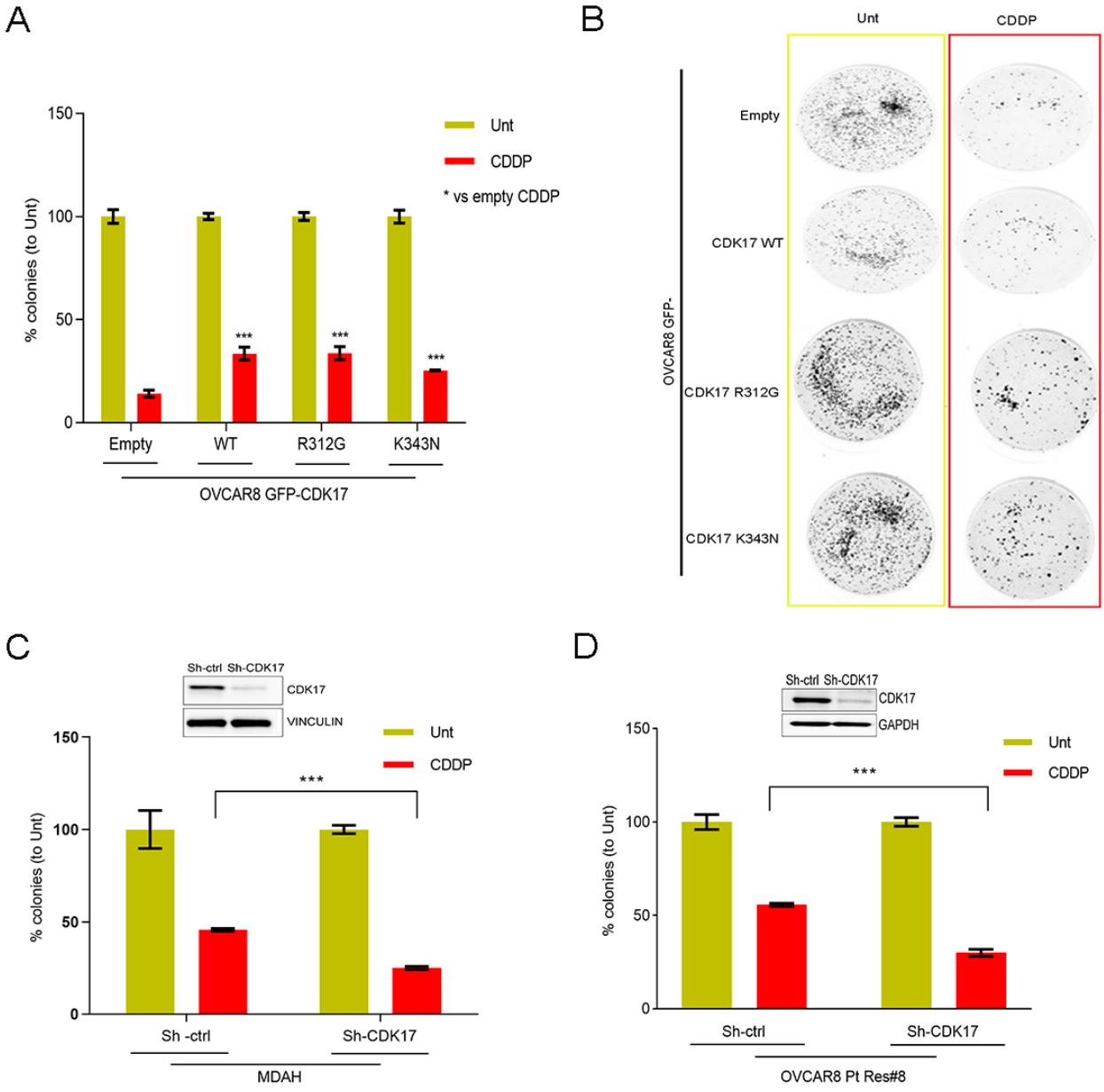

Figure 4.2 CDK17 re-sensitizes PT-resistant cells to CDDP. **A**) On the left, colony assay quantification is graphed as percentage of colonies respect to untreated conditions, as control. **B**), Crystal violet staining of colony assay. OVCAR8 cells, expressing GFP-empty, CDK17 WT, R312G, and K343N constructs were plated in 60 mm plate in triplicate and treated or not with 5 μM CDDP for 6h and fixed after 10 days. Statistical significance was determined by a two-tailed, unpaired Student's t-test (***p<0.001). **C**) Colony assay quantification performed on MDAH cells stably transduced as indicated, treated or not with CDDP. **D**) Colony formation assay on PT-resistant OVCAR8 clone 8 (hereafter OVCAR8 Pt Res#8) stably silenced as indicated, treated or not with CDDP for 6 hours and released; after 10 days cells were fixed and manually counted. In **C** and **D** associated WB displays the expression of cells transduced with the indicated Sh-RNAs. Vinculin and GAPDH were used as loading controls. Graphs represents the mean (± SD) of three independent experiments. Statistical significance was determined by a two-tailed, unpaired Student's t-test (***p<0.001).

We also observed that depletion of CDK17 in OVCAR8 PT-resistant cells, (clone OVCAR8 PT-Res#8) recently generated in our lab, [77] significantly reduces their ability to form colonies after CDDP treatment compared to the control counterpart, suggesting that CDK17 could participate in the definition of a PT-resistant phenotype (Figure 4.2D).

4.2 CDK17 silencing increases DNA-damage in EOC cells

Results from cell viability and colony formation experiments showed that cell lacking CDK17 expression decreased survival and proliferative capacity under PT-exposed conditions. These results could be linked to a different capacity of CDK17 modified cells to repair the DNA damaged by PT treatment. To evaluate if CDK17 participates in PT-induced DNA damage response we performed CDDP time course experiments on OVCAR8 (Figure 4.3A and B) and COV362 (Figure 4.3C and D) cell lines to evaluate the presence of damaged DNA looking at the expression of phosphorylated pS139-γ-H2AX (hereafter γ-H2AX). Using this assay, we showed that CDK17 silenced cells display an increased γH2AX expression at 6 hours and especially after 24 hours after release of PT-treatment, respect to control counterpart (Figure 4.3 A, B, C and D), suggesting that CDK17 could participate to the control of PT-induced DNA damage and/or repair. These data were confirmed by evaluating γ-H2AX expression by western blot analyses in OVCAR8 and MDAH cells treated with CDDP for 6 hours and released, as indicated (Figure 4.3E).

We have already demonstrated that PT-resistant cells are extremely resistant to PT-induced damages.[77] We thus used a CDDP-time course experiments in PT-resistant OVCAR8 PT-Res#8 control and sh-CDK17 to evaluate if CDK17 silencing could modify the response to PT-induced DNA damage, by western blot analysis, also in resistant cells. Strikingly, silencing of CDK17 in PT-resistant cells is associated with increased γH2AX expression, in a time dependent manner as demonstrated by western blot analysis (Figure 4.3F), further highlighting the importance of CDK17

in the response to CDDP-treatment. Interestingly, we also observed that CDK17 expression decreases during the early hours of CDDP treatment and restores its expression after release.

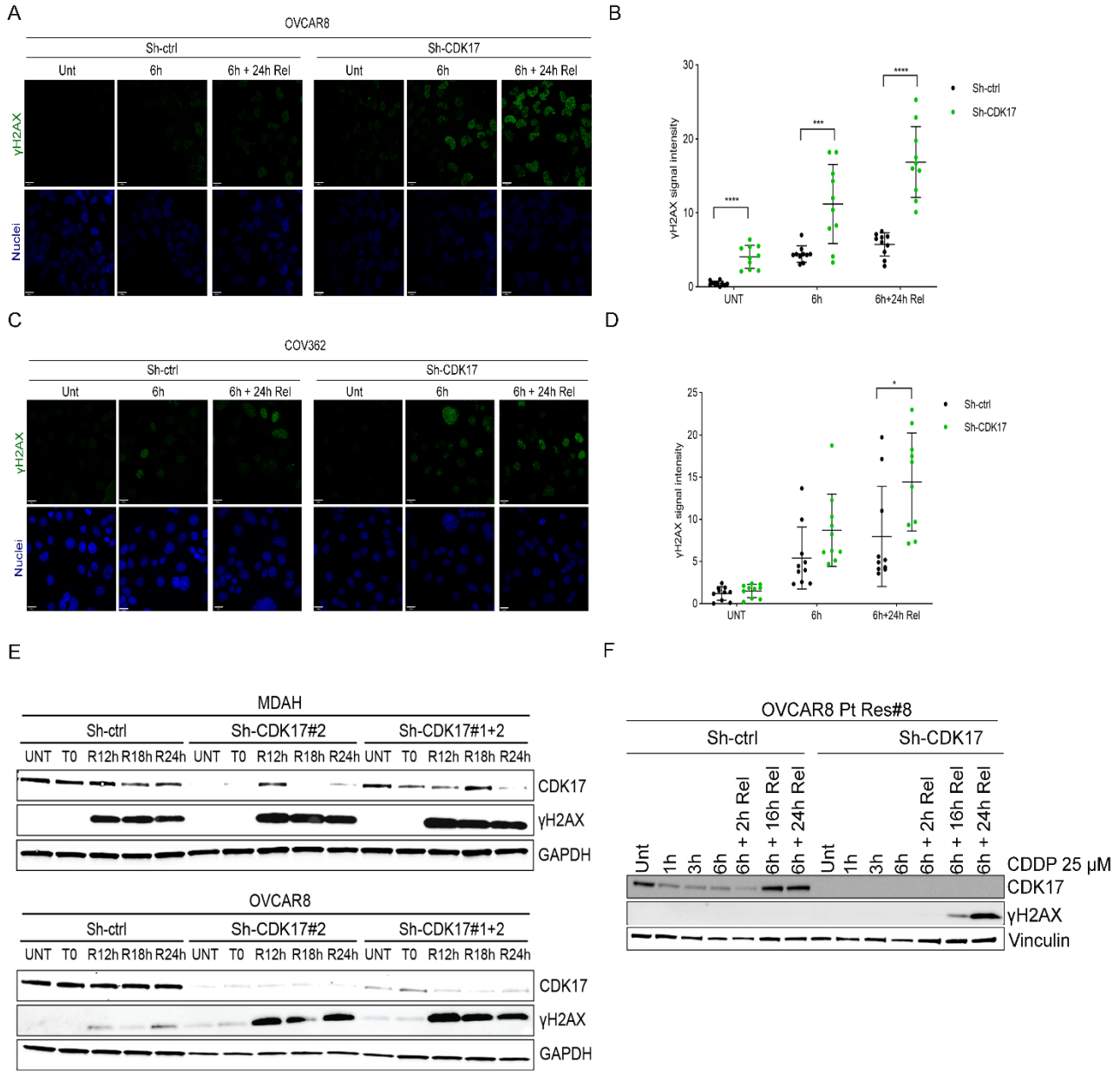

Figure 4.3 CDK17 silencing sensitizes cells to CDDP-induced DNA damage. A) OVCAR8 Sh-ctrl and Sh-CDK17 stably silenced cells were seeded on coverslips and following day treated and collected at indicated time points. Expression of γH2AX is visualized by immunofluorescence (hereafter IF). Signal intensity is quantified, in Fiji software, for randomly chosen 10 cells per time point and graphically showed in **B**). Statistical significance was determined by a two-tailed, unpaired Student's t-test. **C**) IF analysis for γH2AX expression in COV362 Sh-ctrl and Sh-CDK17 stably silenced cells. **D**) Graph shows the quantification of γH2AX signal intensity for randomly chosen 10 cells in **C**). **E)** WB depicting γH2AX expression in OVCAR8 and MDAH control and stably CDK17 silenced cells in time course CDDP treatment. Sh-CDK17 #1+2 indicates the combination of two different CDK17 shRNAs to possibly potentiate silencing,

respect to single shRNA (Sh-CDK17 #2). Also, peculiarly we observed transient increase in CDK17 expression at different time points of the releases in MDAH sh-CDK17 cells, likely due to inefficient silencing. **F)** WB depicting γH2AX expression in PT-resistant OVCAR8 control and CDK17 stably silenced cells in time course CDDP treatment.

4.3 Identification of CDK17 interactome

CDK17 is arguably the least studied member of CDK family and henceforth its interactors are unknown. Therefore, to identify possible CDK17 interactors, we performed unbiased proteomic studies in OVCAR8 cells transiently over-expressing GFP-empty and GFP-CDK17 WT constructs, as described in material and methods. Next, we performed network analysis to visualize connections within our list of proteins. To do so, we mapped our proteome result (log2(fold change (WT vs Empty)) >= 1.0 cut off for a total of 355 proteins) to publicly available protein-protein interaction database BioGrid. Then, in the obtained high dimensional network we applied "Molecular Complex Detection Algorithm" (MCODE) to retrieve the densest cluster (see material and methods) and obtained the network showed in Figure 4.4A. The identified proteins, in this cluster, belong to endocytosis and vesicular trafficking pathways.

Then, to further confirm the reliability of this sub-network analysis and to identify enriched pathways, we performed functional enrichment analysis with whole list of the proteins those had log2(FC) ≥2.0 in our proteome study, using the KEGG-pathway repository. Endocytosis and vesicular trafficking pathway are confirmed, also by KEGG pathway enrichment analysis, to be the most enriched ones (Figure 4.4B). Specifically, 11 out of 126 proteins from our proteomic analysis with log2(FC) >= 2.0, were mapped to endocytosis pathway as reported in Figure 4.4B. Endocytosis is an essential molecular mechanism for cell integrity deeply involved in the control of cancer onset and progression and response to therapies.[90]

As mentioned above, we have included in our study two CDK17 missense mutations (R312G and K343N), identified in ovarian cancer patients. Specifically, R312G mutations alters the HRD motif, that is indispensable for the proper CDKs activation. Moreover consulting COSMIC database, we found that R312G is the most frequently reported compared to K343N mutation,[91] and hence we prioritized R312G mutation, at least in first instance, for further experiments. First, we were interested if and to what extent such mutation would alter wild type CDK17 interactome. To that end, we have performed a second proteome study using the same approach in OVCAR8 cells transiently over-expressing GFP-empty (as negative control), GFP CDK17-WT and CDK17-R312G. Pathway enrichment analysis confirmed also in this case that endocytosis is among the most enriched pathways (data not shown). The comparison between protein bound to CDK17-R312G and CDK17-WT

suggest that this mutation could alter the affinity of some proteins for CDK17, as evidenced in the heatmap shown in Figure 4.4C. Interestingly, both wild-type and mutant CDK17 had similar affinity (peptide counts) toward EGFR protein (Figure 4.4C, red arrow). EGFR executes a plethora of functions under normal and pathological conditions, including cancer progression, being one of the clinically most promising targets. Moreover, EGFR overexpression is reported in some EOC cohorts, and its activation is associated with increased malignant tumour phenotype and poorer patient outcome. More related to this study, several evidence suggest that intrinsic and therapy-induced cellular stress triggers robust, noncanonical pathways of ligand-independent EGFR trafficking and signaling, which provides cancer cells with a survival advantage and resistance to therapeutics.[92] Besides, in our first proteomic study we found that AP2A2 and EPS15 were among top enriched proteins (Figure 4.4A) and it is known that the interplay between these two proteins decide the fate of internalized EGFR toward a degradation route if EPS15 alone bound to EGFR, or a recycling endocytosis when EPS15-AP2A2 are both present in the complex.[93] Based on these results, we hypothesized that CDK17 might cooperate with AP2A2 and EPS15 proteins in regulating EGFR endocytosis.

First, we checked the mutational status of CDK17, EGFR and the 11 endocytosis proteins, obtained by our previous analysis, in Cancer Cell Line Encyclopaedia database. Results related to EOC cell lines are graphically summarized in (Figure 4.5A). CDK17 is mutated only in COV362 cell line (G406R), together with EGFR (H112Q) and ASAP1 alterations (E588Afs*33 and amplification) (Figure 4.5A). EGFR (R255Q) is also mutated in CAOV3 and present deep deletion in SKOV3 cell lines. EPS15 does not have any genetic alterations in our EOC panel and AP2A2 showed deep deletions in COV318 and OV90 cell lines. WASHC5 and ASAP1 were the most altered genes in the analysed EOC cells lines generally due to genes amplification (Figure 4.5A).

At the same time, we evaluated the protein expression of a subset of these genes in the same EOC cell lines panel (Figure 4.5B). CDK17, that has never been specifically investigated for its expression in EOC before, EPS15 and EGFR are easily detectable in almost all cell lines tested; only TOV112D does not express EGFR protein and express EPS15 at lower levels respect to other EOC cell lines (Figure 4.5B). Then, we performed the same evaluation in a panel of PT-resistant cell lines (Figure 4.5C). To better visualize if expression status of these 3 proteins was different between parental and resistant cell lines, we used an heatmap representation of their expression normalized to loading controls (Figure 4.5D). We did not notice major differences in the expression status of EPS15 and EGFR proteins between parental and resistant cells. Conversely, CDK17 expression seems slightly

increased in resistant cell lines compared to parental counterparts (Figure 4.5D). More studies on different models, cell clones and human cancer samples are necessary to confirm this tendency.

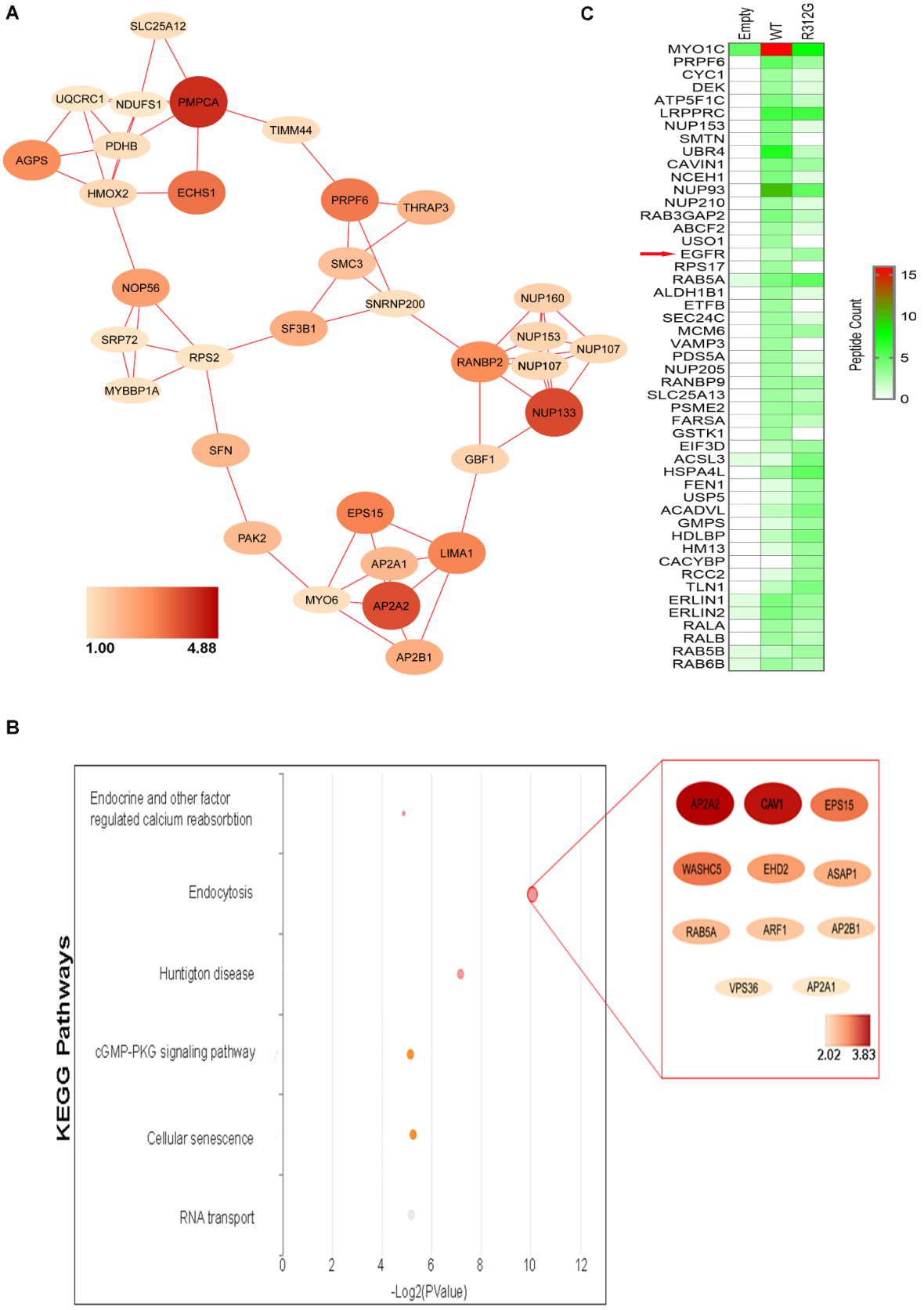

Figure 4.4 CDK17 interactome includes endocytosis and vesicular trafficking pathways. A) OVCAR8 cell expressing GFP-empty or GFP-CDK17 were pulled down in triplicate, using GFP-trap approach and Mass-Spectrometry analysis was performed. Obtained list of enriched proteins was mapped to Biogrid,[94] to generate first a general "connectome" and by MCODE a more defined clustered network was obtained.[85] Dimension and colouring of nodes are according to their Log2(FC(GFP-CDK17 vs GFP-empty). **B)** KEGG pathway enrichment analysis was performed with proteins that had at least log2(FC) ≥2. Endocytosis was predicted as the most enriched pathway followed by Huntington disease. **C)** Heatmap representing the most enriched proteins, obtained by Mass Spectrometry peptide count, in CDK17 WT and R312G mutant versus GFP empty expressing cells, used as negative control. EGFR is highlighted by red arrow. Generally, compared to CDK17 WT, CDK17 R312G presents reduced affinity to SMTN, USO1, ETFB, GSTK1D proteins; on the other hand, it has increased affinity toward CACYP and HM13 proteins, suggesting at least partially impact of this mutation on CDK17 interactome.

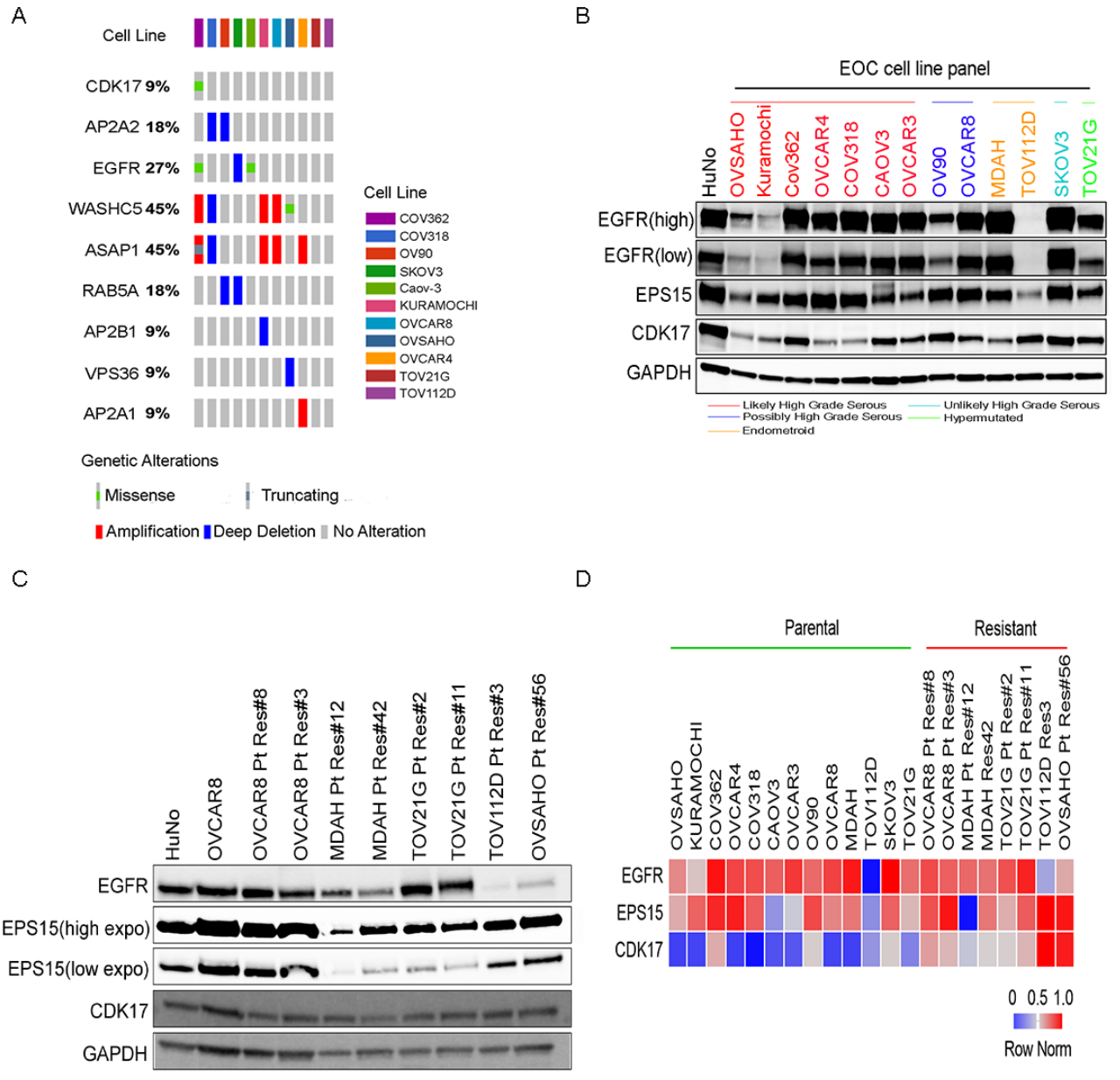

Figure 4.5 CDK17 is well expressed in a panel of parental and PT-resistant EOC cell lines A) Copy Number Variation (CNV) and mutational status were retrieved from Cancer Cell Line Encyclopaedia (Broad Institute)[95] and visualized using Bioconductor, Complex-Heatmap package, Oncoprint function.[87] **B**) WB representing expression profile of EGFR, EPS15 and CDK17 in EOC cell line panel. **C**) WB analysis of EGFR, EPS15 and CDK17 in EOC PT-resistant cell lines. **D**) Heatmap visualization of expression status of EGFR, EPS15 and CDK17 in parental and resistant cell lines. Quantification of bands from **B** and **C** were normalized to the mean (Human Normal, HuNo in B and in C) of respective HuNo bands and then log transformed and represented as row-wise normalized data. For OVCAR8 quantified bands were taken from the gel in **B**.

Next, to validate proteomic results, we performed co-immunoprecipitation (co-IP), experiments looking at the interaction between endogenous CDK17 and EGFR in OVCAR8 cells, both in basal and PT-treated conditions. By immunoprecipitating CDK17, despite decreased CDK17 expression at 1 and 3h of CDDP treatment, we appreciated a CDK17-EGFR interaction in untreated conditions that seemed to be further strengthened after CDDP-treatment (Figure 4.6A). These data were confirmed by immunoprecipitating EGFR and looking at the presence of co-IP CDK17 in the same lysates (Figure 4.6B).

We also confirmed the interaction between CDK17 and AP2A2, which was among the most enriched proteins in GFP-CDK17 WT versus GFP-empty Mass-Spectrometry analysis (Figure 4.4C) and that is involved in EGFR recycling.[96] Interestingly, using the 6 hours' time point of CDDP treatment we observed that PT-treatment increased the interaction between AP2A2 and CDK17 either by IP CDK17 and by IP AP2A2 Figure 4.6C and 4.6D. Similar results were obtained looking at the interaction between EPS15 and CDK17, that was confirmed in basal condition and after CDDP treatment but the interaction modulation by PT-treatment seemed less evident and merits further confirmation (Figure 4.6D and 4.6E).

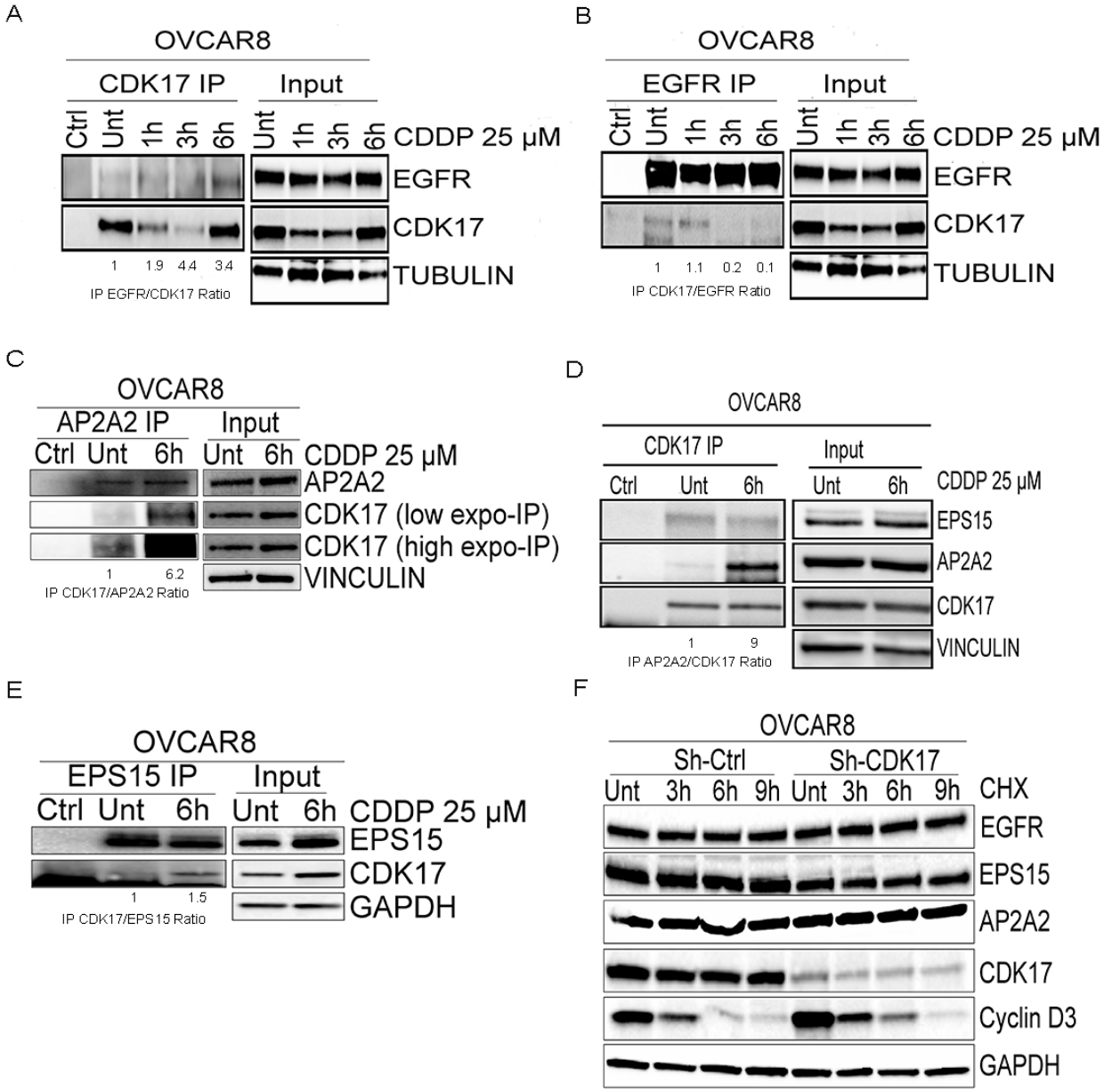

Figure 4.6 CDK17 binds to endogenous EGFR and EGFR-interacting partners. A) and **B**) Co-IP analyses (CDK17 and EGFR IPs, respectively) in OVCAR8 cells, treated or not with CDDP 25 µM at indicated time points. Input reports the expression of the indicated protein in the lysates used for IPs experiments. Tubulin was used as loading control. Densitometric analysis of the IP ratio is reported under the blot. **C**) and **D**) OVCAR8 cells were treated or not with CDDP 25 µM for 6 hours and obtained lysate were pulled down with AP2A2 antibody (C) and CDK17 (D) antibody respectively. **E**) OVCAR8 cells were treated or not with CDDP 25 µM for 6 hours and obtained lysate were pulled down with EPS15 antibody. **F**) Cycloheximide (CHX) time course experiment in OVCAR8 cells stable silenced or not for CDK17. Cyclin D3 was used as read out for effectiveness of CHX treatment.

4.4 CDK17 is involved in EGFR-uptake and internalization mechanisms

To understand if CDK17 had any effect on EGFR signalling we first evaluated if it could have any impact on the stability of EGFR, EPS15 or AP2A2 proteins. Using cycloheximide (CHX) to block de novo protein synthesis we, however, did not observed any differences in EGFR, EPS15 or AP2 total protein stability between control and CDK17 silenced OVCAR8 cells, at least in basal conditions (Figure 4.6F).

Next, we investigated if CDK17 could modulate EGFR activation and trafficking, looking at the expression and localization of active (pY1068)-EGFR in serum starved cells stimulated for 5 minutes with 20 ng/ml of EGF and then released in EGF free medium for up to 20 minutes using immunofluorescence analysis (see Material and Methods section). As shown in Figure 4.7, despite having equal levels of phosphorylated EGFR after starvation, EGF-stimulation leads to higher phosphorylation of EGFR in OVCAR8 control cells compared to cells silenced for CDK17, starting from 10 minutes after the release from EGF stimulation. Zoomed areas (Figure 4.7B) clearly showed the differences in pY1068-EGFR expression and localization, being more present and more diffuse in cytoplasmic vesicles in control than in CDK17 silenced cells. In these latter cells pY1068-EGFR tend to accumulate in perinuclear areas usually defined as "endosomal sorting complex" where sorting of cargo takes place, either send to degradation in lysosomes or recycled/re-distributed. [97–99] Apparently, at later time points, especially at 20 minutes, in sh-CDK17 cells, perinuclearly accumulated pY1068-EGFR signal seems to disappear or to be degraded. On the other hand, in control cells pY1068-EGFR signal persists (Figure 4.7B, see T20 zoom-in). These results suggested that the presence of CDK17 can somehow contribute to loading active-EGFR to vesicles, and likely prevents EGFR from being sorted into a degradative path.

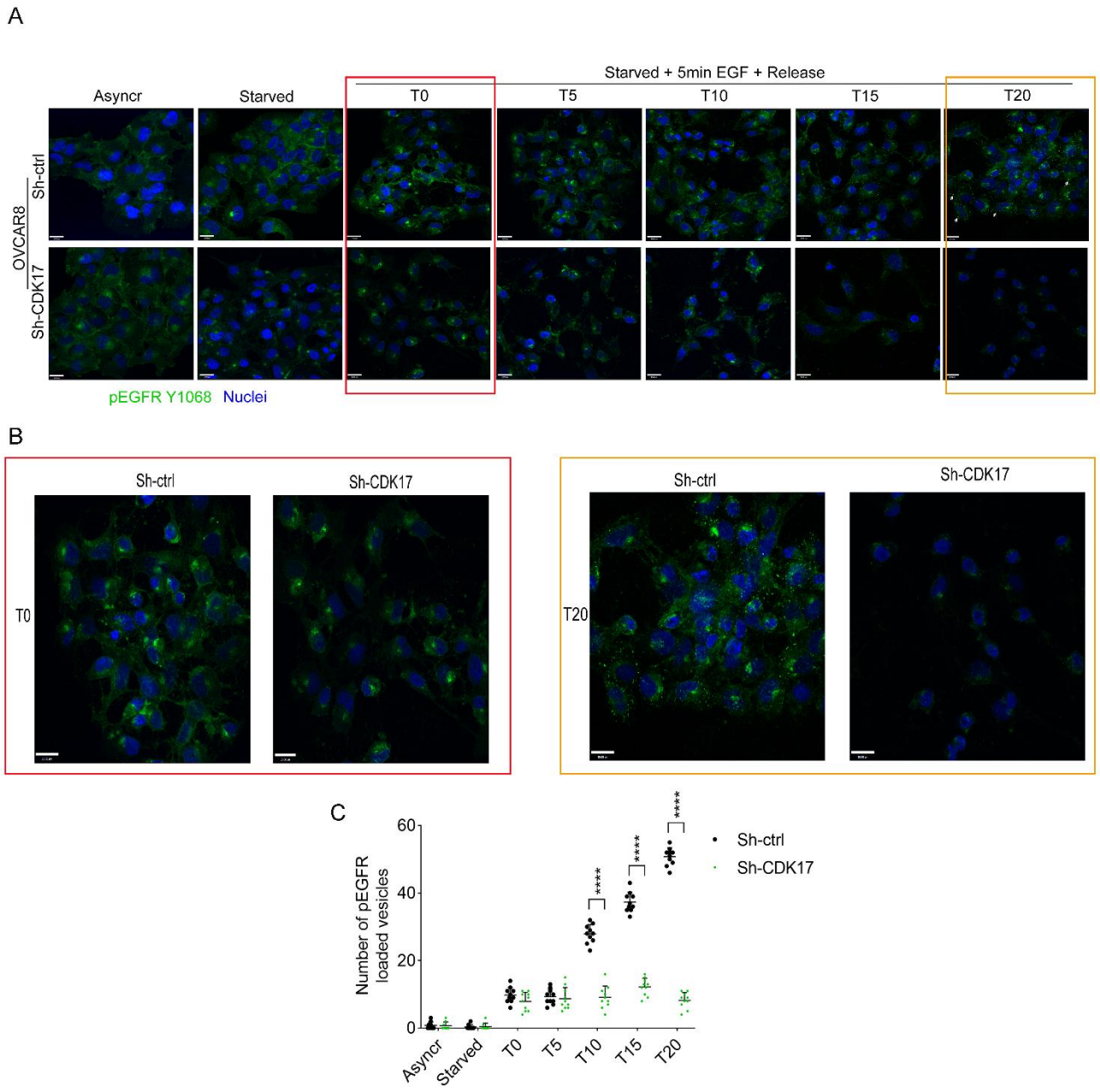

Figure 4.7 CDK17 protects internalized active EGFR from degradation. A) IF analysis evaluating pEGFR Y1068 (green) localization and expression in OVCAR8 cells stably transduced with the indicated Sh-RNAs. Starved cells were stimulated with EGF and then released and prefixed at indicated time points. Nuclei were stained with TO-PRO (pseudo-colored in blue). Scale bar= 18µm. **B**) Zoom-in view of T0 in red frame. In orange frame depicted zoom-in view of T20. As shown, at later time points pEGFR Y1068 content diminished in OVCAR8 Sh-CDK17 cells. In OVCAR8 Sh-ctrl cells pEGFR Y1068 persists at time T20, notably most of the content is compartmentalized. Scale bar= 18µm. **C**) Graph represents the mean count of pEGFR Y1068 positive vesicles in randomly chosen 10 cells per time-point. Statistical significance was determined by a two-tailed, unpaired Student's t-test.

4.5 CDK17 silencing reduces vesicle loading of EGFR

Based on these results, we analysed more in detail the activation and localization of pY1068-EGFR in cells silenced or not for CDK17 and then stimulated with EGF first looking at its localization in early endosome, marked by the expression of the EEA1 (Early Endosome Antigen 1) protein. In this case we decided to use PT-Resistant cells to verify if the difference in EGFR activation was maintained also in this context. To this aim, we starved OVCAR8 Pt Res#8 Sh-ctrl and Sh-CDK17 and stimulated with EGF. Serum starved OVCAR8 Pt Res#8 Sh-ctrl and Sh-CDK17 have low levels of EGFR activity (Figure 4.8A). Five minutes of EGF stimulation results in slightly higher pY1068-EGFR levels in Sh-ctrl cells compared to Sh-CDK17 cells and these differences become more evident and significant at later time points, suggesting that CDK17 modulates EGFR also in the context of PT-resistance. We also noticed that, at late time points after stimulation, the remaining pY1068-EGFR content is largely compartmentalized into either EEA1-positive (orange dots/aggregates) or EEA1-negative vesicles (green dots/aggregates) (Figure 4.8A and B). Counting pY1068-EGFR positive vesicles (green dots), we confirmed the highest differences between control and CDK17-silenced cells especially at the 20 minutes time point (Figure 4.8C). Moreover, we also quantified pY1068-EGFR-EEA1 colocalization using the Volocity computer program and verified a higher Pearson colocalization coefficient score in control than silenced cells (Figure 4.8D). Yet we cannot exclude those differences in co-localization between EEA1 and pY1068-EGFR could be due to the different activation of EGFR in CDK17 silenced cells and thus this possibility should be confirmed in future analyses. Nevertheless, we noticed that in CDK17 silenced cells EEA1 positive vesicles tend to accumulate perinuclearly, an observation not evident in control cells (Figure 4.8A-B), suggesting that CDK17 could effectively affect endosome recycling.

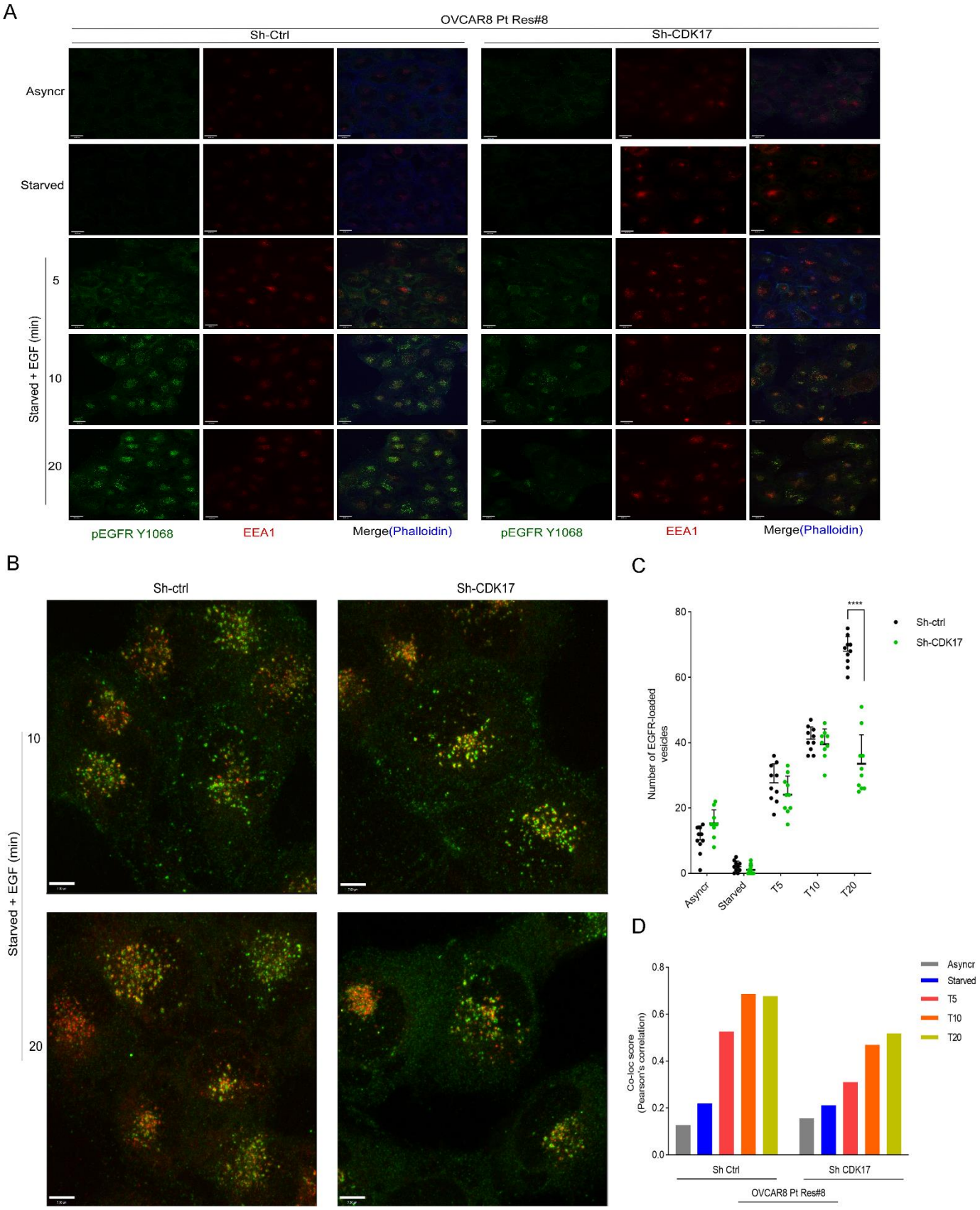

Figure 4.8 CDK17 silencing decreased pEGFR Y1068 expression its endosomal localization. A) OVCAR8 PTRes#8 Sh-ctrl and Sh-CDK17 were starved for 24 hours, then stimulated with 20 ng/mL of EGF for indicated time points. IF analysis evaluated pEGFR Y1068 (green) and EEA1 (red) localization and expression at indicated conditions. Scale bar=

18.00 µm. **B**) Z-axis view of pEGFR Y1068 and EEA1 colocalization. Scale bar = 7.00 µm. **C**) Number of pEGFR Y1068 positive vesicles (green dots) were counted in randomly chosen 10 cell per condition, using Fiji software.[83] . Statistical significance was determined by a two-tailed, unpaired Student's t-test **D**) pEGFR Y1068 and EEA1 colocalization was quantified with Fiji software, represented as Pearson correlation coefficiency score.

4.6 CDK17 is involved in the sustainment of EGFR signalling

The data collected with IF analyses suggested that EGFR activity is differently regulated in CDK17 silenced cells and in particular that even if EGFR is equally activated upon stimulation with its ligand EGF, its active phosphorylated form persist longer when CDK17 is expressed.

To confirm this possibility, OVCAR8 control (Sh-ctrl) and CDK17-silenced cells (Sh-CDK17) were starved, treated with cycloheximide (CHX) and stimulated with EGF, for the indicated time points (Figure 4.9A). This approach demonstrated that CDK17 silencing destabilizes pY1068-EGFR levels, respect to control cells, particularly evident at 30-45 minutes after EGF stimulation, in line with the differences noted with IF analyses. Accordingly, the inhibition of ubiquitin mediated proteasomal degradation, using MG132 resulted in higher accumulation of degraded pY1068-EGFR in cells silenced for CDK17 compared to control cells, indicating that, in the absence of CDK17, activated EGFR more actively degraded through proteasome activity (Figure 4.9B).

To understand to what extent CDK17 contribute to maintain EGFR signalling in an activated state, we stimulated OVCAR8 Sh-ctrl and Sh-CDK17 cells with 20 ng/mL EGF for 5 minutes and released the cells in EGF free medium for different time points. As shown in (Figure 4.9C) both in control and CDK17-silenced cells, phosphorylation of EGFR is similar at 5 minutes of stimulation. Interestingly, while in control cells pY1068-EGFR expression remained sustained for up to 30 minutes after the release, in CDK17 silenced cells it diminished sharply, as early as 5 minutes after the release (Figure 4.9C). These data were then confirmed in control and CDK17 silenced PT-Resistant OVCAR-8 cells stimulated with EGF for up to 30 minutes (Figure 4.9D). Finally, we evaluated the extent of EGFR pathway activation upon EGF stimulation in cells over-expressing CDK17-WT or CDK17-R312G respect to EGFP expressing control cells. In this case EGF stimuli was maintained for up to 45 minutes. In these conditions CDK17-R312G mutant not only maintained high levels of pY1068-EGFR expression throughout stimulation times, but also resulted in a higher expression of Akt and ERK activating phosphorylation (Figure 4.9E). Collectively these results showed that CDK17 expression and activity is necessary for the sustained EGFR signalling over time.

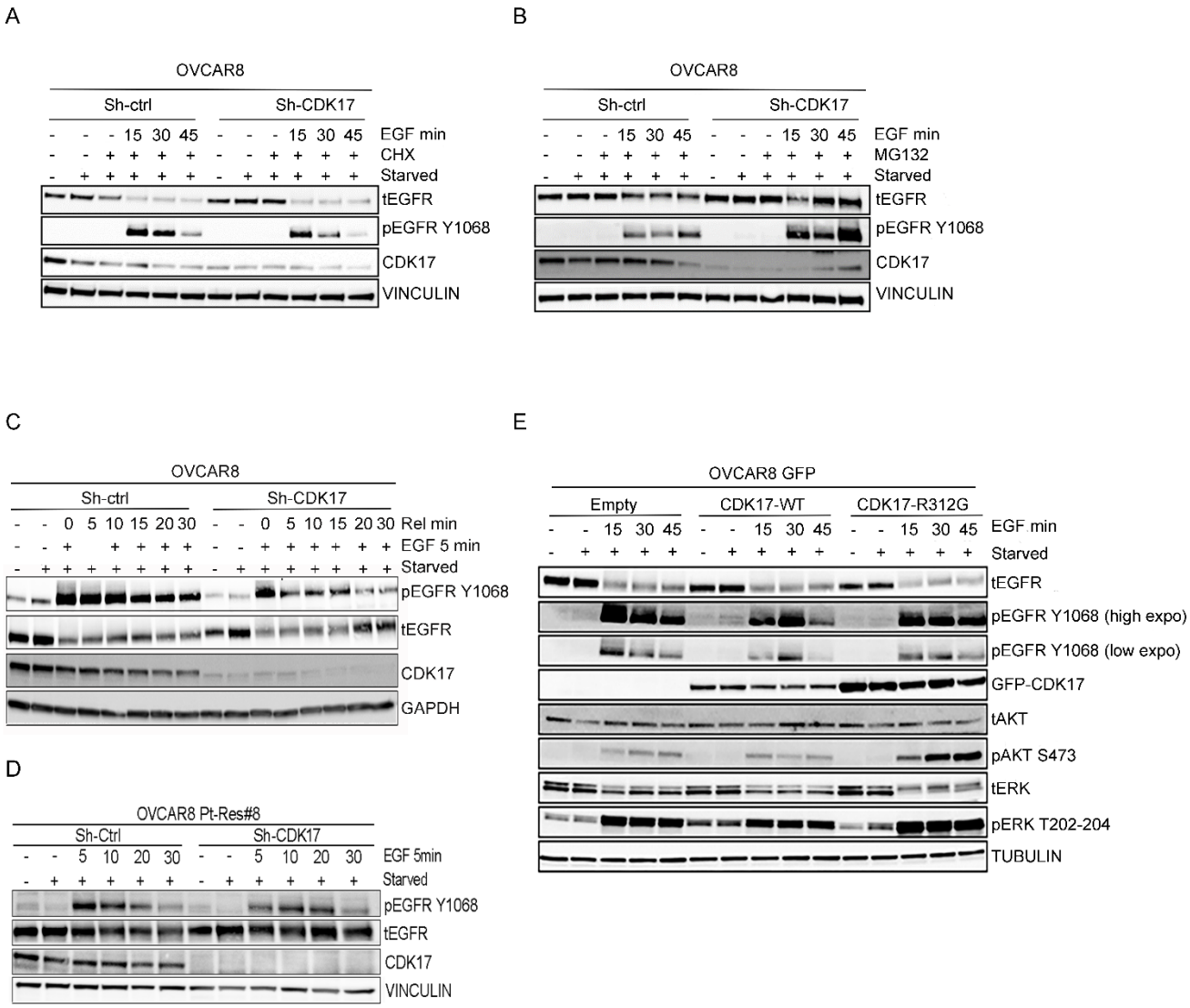

Figure 4.9 CDK17 sustains EGFR signalling over time. A) WB analysis of OVCAR8 Sh-ctrl and Sh-CDK17 cells, starved, stimulated with EGF and treated with CHX at indicated time points. Vinculin was used as loading control. **B**) Starved OVCAR8 Sh-ctrl and Sh-CDK17 cells were pre-treated with MG132 to block proteosome before stimulating cells with EGF. MG132 pre-treatment causes higher accumulation of degraded pEGFR Y1068 in OVCAR8 Sh-CDK17 cells compared to its control counterpart. Vinculin was used as loading control. **C**) Starved OVCAR8 Sh-ctrl and Sh-CDK17 cells were stimulated with 20 ng/mL of EGF for 5 minutes and then released for indicated time points. GAPDH was used as loading control. **D**) PT-resistant OVCAR8 cells silenced or not for CDK17 were starved for 24 hours and stimulated with 20ng EGF for indicated time points. Vinculin was used as loading control. **E**) OVCAR8 cells stably overexpressing GFP-empty, GFP-CDK17 WT and GFP-CDK17 R312G mutant constructs were stimulated with 20 ng/ml EGF for indicated time points, after starvation. Tubulin was used as loading control.

4.7 CDK17 is involved in non-canonical phosphorylation of EGFR upon CDDP exposure

Literature data reported that stress conditions, such as CDDP treatment and/or radiation therapy, induce a noncanonical EGFR phosphorylation, in particular at Ser1015, Ser1047 and Threonine 669, via p38 activation, which lead to compartmentalization of EGFR, causing chemo- and radio-resistance. [100,101] Since CDK17 seemed to be involved in the sustainment of EGFR signalling and modulated PT-response in EOCs, we investigated the role of CDK17 in regulating EGFR activation upon CDDP treatment. Previous report suggested that CDDP induces canonical EGFR activation in EOC cell lines.[102] However, in our experiments with CDDP in OVCAR8 and MDAH cells we did not observe a modified pY1068-EGFR phosphorylation under CDDP treatment during the first 6 hours of treatment (Figure 4.10A). Yet, by performing longer time point experiment including the release from CDDP treatment we observed an increased pY1068-EGFR expression 16-24 hours after CDDP removal in a number of EOC cell lines (Figure 4.10B-D). These data suggest that in our models CDDP does not directly influence pY1068-EGFR phosphorylation and is in line with recent reports showing that CDDP treatment, like other stress conditions such as UV, triggers EGFR by inducing its Serine/Threonine (Ser/Thr) phosphorylation and depends on EGFR internalization and intracellular retention.[103] EGFR signalling from intracellular vesicles then delays apoptosis and might contribute to chemoresistance.[101] In particular it has been proposed that upon several stresses including CDDP treatment, EGFR is phosphorylated on Ser 669 (pS669-EGFR).[104] We thus tested the expression of pS669-EGFR in control and CDK17 silenced cells treated with CDDP for up to 6 hours. Our data demonstrated that CDDP treatment rapidly increased pS669-EGFR expression but that its expression was not decreased and rather increased by CDK17 silencing in OVCAR8 cells (Figure 4.10E), suggesting that CDK17 did not directly phosphorylated EGFR at S669. Yet, as CDK17 being a Ser/Thr kinase, we next tested if it may influence non-canonical Thr/Ser EGFR phosphorylation under CDDP treatment on a yet to be identified residue. To this aim we IP total cell lysate from control and silenced OVCAR8 cells treated or not with CDDP for 6 hours, with generic anti phospho-Thr (pThr) or phospho-Ser (pSer) antibodies. IP proteins were then evaluated for the presence of EGFR in western blot analyses. Results showed that, upon CDDP treatment, in control cells EGFR was readily found in anti-pThr IP and, more importantly, that its expression sharply decreased in anti-pThr IP from CDK17 silenced cells (Figure 4.10F). Conversely CDDP treatment did not significantly modified the amount of pSer IP EGFR in control cells while decreased it in CDK silenced cells (Figure 4.10F). This observation shows that CDK17 is necessary for EGFR Thr phosphorylation induced by PT treatment. Our result also shows that CDK17 expression is relatively

high in Sh-ctrl CDDP-treated cells and that is associated with higher phosphorylation of EGFR at its Threonine residue(s) (Figure 4.10F). Trying to clarify the possible significance of CDDP-induced Thr phosphorylation of EGFR we next looked at the expression of EGFR in control and CDK17 silenced cells treated or not with CDDP. As positive control for this experiment we used Cetuximab (CTX), a well-known EGFR-monoclonal antibody that triggers EGFR internalization and degradation, which was also shown to cooperate with chemotherapy to induce immunogenic cell death in colorectal cancer.[105,106] Our data showed that in control cells CDDP and Cetuximab treatment reduced EGFR protein levels to a similar degrees (Figure 4.10G and H) and combination treatment was more potent compared to either alone (Figure 4.10G and H). Moreover, in CDK17 silenced cells both CDDP and to a lesser degree, Cetuximab treatments were more effective in reducing EGFR protein levels compared to control cells (Figure 4.10G and H). Last but not the least, in sh-CDK17 cells EGFR degradation was more pronounced under combination treatment respect to control cells (Figure 4.10G and H). These data along with the above reported experiments showing no effects of CDK17 on the expression and protein stability of EGFR in untreated cells (Figure 4.6D), suggest that CDK17-mediated EGFR phosphorylation on a Thr residue could be important to sustain its expression under stress conditions.

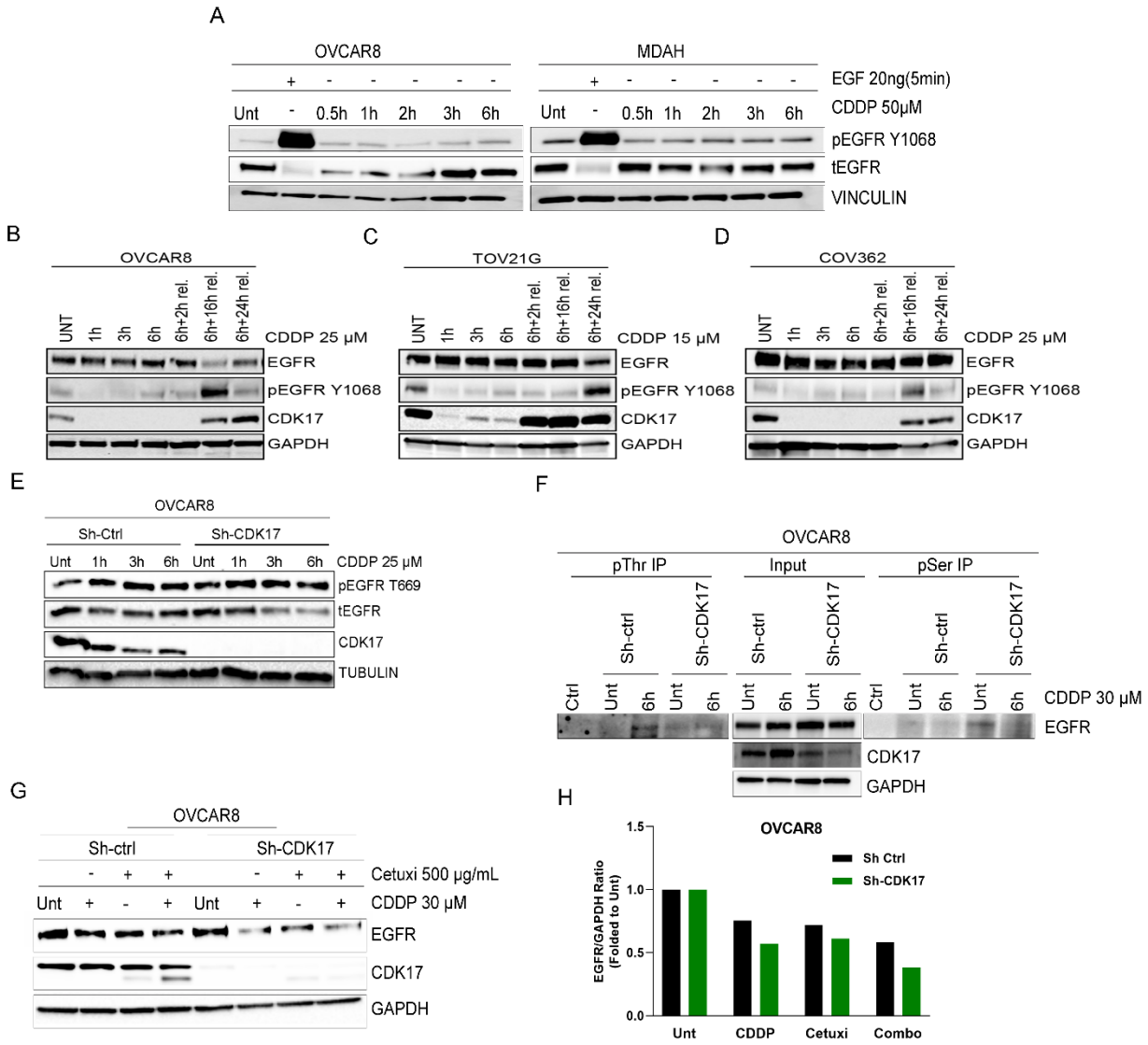

Figure 4.10 CDK17 likely promotes non-canonical phosphorylation of EGFR protein under CDDP treatment. A) CDDP time course experiment on OVCAR8 and MDAH cell lines. EGF stimulation was used as a positive control to see whether CDDP induces canonical, ligand induced, EGFR phosphorylation. Vinculin was used as loading control. **B-D)** OVCAR8, TOV21G and COV362 EOC cell lines were challenged with CDDP and then released as indicated. Not CDDP treatment but release from CDDP resulted in phosphorylation of EGFR at Threonine 1068 in all EOC cell lines, specifically at later release time points. GAPDH was used as loading control. **E)** CDDP time course experiment to evaluate whether CDK17 is involved in the phosphorylation of EGFR at Threonine 669 residue or not. Tubulin was used as loading control. **F**) Lysate of OVCAR8 Sh-ctrl and Sh-CDK17 cells treated or not with CDDP for 6 hours were pulled down with total pThreonine (pThr) and pSerine (pSer)antibodies. Input reports the expression of the indicated protein in the lysates used for IPs experiments. GAPDH was used as loading control. **G**) OVCAR8 Sh-ctrl and Sh-CDK17 cells were treated with CDDP and Cetuximab alone 1 hour or in combination (1h CDDP+1 h Cetuximab). GAPDH was used as loading control. **H)** Quantification of EGFR bands in G), normalized to GAPDH expression.

4.8 CDK17 promotes AP2A2-EPS15 interaction under CDDP treatment

The above results (Figure 4.10A and 4.10B) demonstrated that in EOC cells CDK17 might be involved in noncanonical phosphorylation of EGFR likely to maintain EGFR protein expression under stress conditions (Figure 4.10C). In physiological conditions EGFR could have different destinies, depending on which of the adaptor interacting proteins is present. Indeed, in the absence of AP2A2, internalized EGFR is lead to degradation, through adaptor proteins, like EPS15 and Epsin.[93] Both AP2A2 and EPS15 were among the top enriched proteins in EGFP-CDK17 pull down proteomic analysis (see Figure 4.4A and B). We thus asked if CDDP treatment could modify their interaction in a CDK17-dependent manner. To test this hypothesis, we IP EPS15 from control and CDK17 silenced cells under basal and CDDP-exposed conditions. As shown, (Figure 4.11A) both CDK17 and AP2A2 co-immunoprecipitated with EPS15 and these interactions were further enhanced by CDDP treatment. Strikingly, silencing of CDK17 abrogates the interaction between EPS15-AP2A2 both in untreated and CDDP-treated cells (Figure 4.11A), suggesting that CDK17 is necessary for the formation of AP2-EPS15 complex that protects EGFR from degradation in stress conditions, such as PT treatment. These results are in line with the observations showing that CDK17 interacts with EGFR (Figure 4.6A), AP2A2 (Figure 4.6C-D) and as well as EPS15 and that all these interactions were further enhanced by CDDP-treatment (Figure 4.6E and Figure 4.11A). Collectively, these results depict a possible role of CDK17 in regulating both ligand - and stress-induced EGFR internalization favouring the use of a non-degradative endocytosis route, as schematically depicted in (Figure 4.11B).

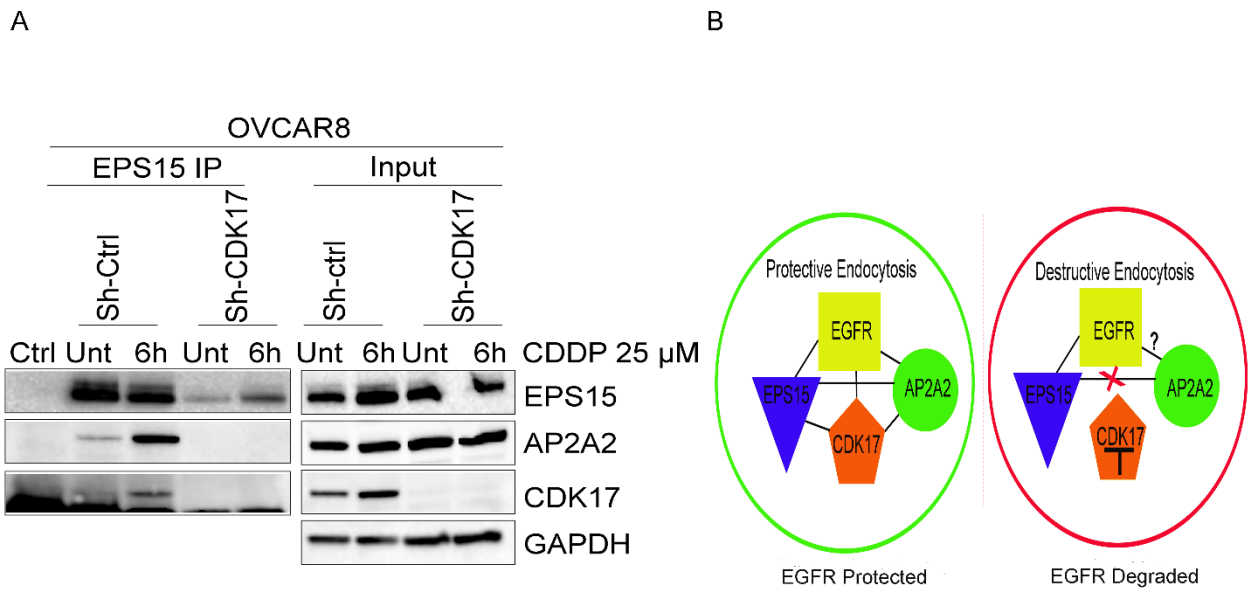

Figure 4.11 CDK17 regulates EPS15-AP2A2 interaction. A) OVCAR8 Sh-ctrl and Sh-CDK17 cells treated or not with CDDP for 6 hours and immunoprecipitated with EPS15 antibody. Input reports the expression of the indicated protein in the lysates used for IPs experiments. GAPDH was used as loading control. **B**) Proposed models showing the multi-directional interaction between CDK17, EGFR, EPS15 and AP2A2. In the presence of CDK17 the interaction of EGFR with the AP2-EPS15 complex favours its recycling and intracellular signals (Protective Endocytosis). When CDK17 is absent/inhibited AP2 does not proficiently bind to EPS15, favouring EGFR pathway to degradation (Destructive Endocytosis).

4.9 CDK17 is kinase active and, potentially, is different from canonical CDKs

Our data indicate that CDK17 might have a kinase activity (Figure 4.10F) and it is accepted that CDKs to exert their kinase activity must be activated, canonically by cyclins. Members of PCTAIRE family, as CDK16, was shown to be activated by cyclins (specifically cyclinY, hereafter CCNY) in conjunction with co-activators, like 14-3-3 proteins. Although a direct interaction between CDK17 and CCNY has never been demonstrated yet, an active CDK17-CCNY complex is commercially available. So, we decided to perform an *in vitro* cell-free kinase assay with the recombinant CDK17-CCNY complex to verify it could phosphorylate in vitro EGFR, EPS15 the AP2 complex. Indeed, the AP2 complex is a heterotetramer consisting of two large adaptins (α and β), a medium adaptin (μ), and a small adaptin (σ): Complex 2 is formed by the AP2A1 (α unit 1), AP2A2 (α unit 2), AP2B1 (β unit), AP2M1 (μ unit) and AP2S1 (σ unit) proteins. Although the AP2A2 subunit was not commercially available we could obtain and use in the in vitro kinase assay the AP2B1 and AP2M1 recombinant proteins; of note, AP2M1 was found enriched in our proteome analysis in CDK17

overexpressing cells (Figure 4.4). Results from this in vitro kinase assay demonstrated that CDK17-CCNY active complex undergo to an auto-phosphorylation and readily phosphorylates both EGFR, and AP2B1 protein (Figure 4.12A, indicated by arrows). While AP2M1 seems not be target of CDK17 kinase activity, when EPS15 was used as substrate we only seen a faint phosphorylated band of the expected molecular weight at 24 hours of exposition (see arrow in Figure 4.12A, 24 hours exposition). Yet we also observed a clear and intense band of a higher molecular weight (Figure 4.12A, indicated by asterisk), that could be the results of an hyperphosphorylated form of EPS15. More experiments are necessary to confirm this possibility. These experiments on one side confirm that CDK17 could directly interact with and phosphorylate EGFR and the AP2 complex, on the other rise some concerns on the fact that in mass spectrometry analysis of CDK17 interactome we did not identify CCNY or any other cyclins. This point should be of course better investigated in the future and we can only make some hypothesis to explain the discrepancy between proteome and kinase assay results: 1) CDK17/CCNY interaction is weak and/or require additional post translational modification that prevent to demonstrate it in basal condition; 2) the EGFP-tag impedes the binding between CCNY and tagged CDK17; 3) CDK17 and/or CCNY had a particular subcellular distribution/localization that decrease the possibility we were not able to detect CDK17-CCNY interaction with our whole cell lysate experiments 4) Although an active CDK17 could phosphorylate in vitro EGFR and AP2, in vivo in EOC cells CDK17 may have different structural configuration and in the absence of CCNY it is available for other activating partners. Additional experiments are in progress to verify if by changing lysis buffer stringency, cells treatment conditions (e.g., CDDP treatment), using different tagged (e.g., Flag or Myc tags) or untagged CDK17 proteins it will be possible to demonstrate a direct interaction between CCNY and CDK17 and EGFR recycling machinery.

In the meantime, we started to investigate the cellular distribution of CDK17 and CCNY performing cell-fractionation experiment. Our results clearly demonstrated that while CDK17 has a homogenous cellular distribution, CCNY is mostly localized to plasma membrane and organelles, and it is almost absent in the cytoplasm (Figure 4.12B). It is thus possible that CDK17 interacts with CCNY only when located in specific subcellular compartments.

Although, specific sub-cellular localization of CCNY could, at least partially explains why we did not identify it in the CDK17 proteome we also conducted 3D configuration analyses of CDK17 starting from the notions that: 1) mutating CDK16 PCTAIRE to PSTAIRE does not change its affinity toward CCNY and 2) CCNY alone is not able to fully drive CDK16 kinase activity.[48] In light of these information, we hypothesized that CDK17, as well as CDK16 may have a different 3D configuration

from canonical CDKs, and do not solely rely on cyclins for their activation. To dissect this aspect, we compared the 3D structure of CDK17 with its closest homolog CDK16 and with the structures of cyclin-bound and cyclin-free CDK1 (used as the reference of "canonical" CDK, activated by cyclins). CDK17 structure is not experimentally resolved. Therefore, we first homology modelled CDK17 structure using as template CDK16 [PDB:5G6V] and then performed structure matching. Interestingly, this comparison revealed that the PCTAIRE domain of CDK16 and CDK17, spatially overlaps well with the cyclin-bound PSTAIRE of CDK1 but not with the CDK1 cyclin-free conformation (Figure 4.12C). Then, we compared CDK16 with the other two members of the PCTAIRE family, CDK5 and CDK18. Interestingly, we found that the cyclin binding domains of CDK5 and CDK18 do not share the same geometry with CDK16 and CDK17 (Figure 4.12D), overall suggesting that specifically CDK16 and CDK17 PCTAIRE could be active also in the absence of a specific bound cyclin.

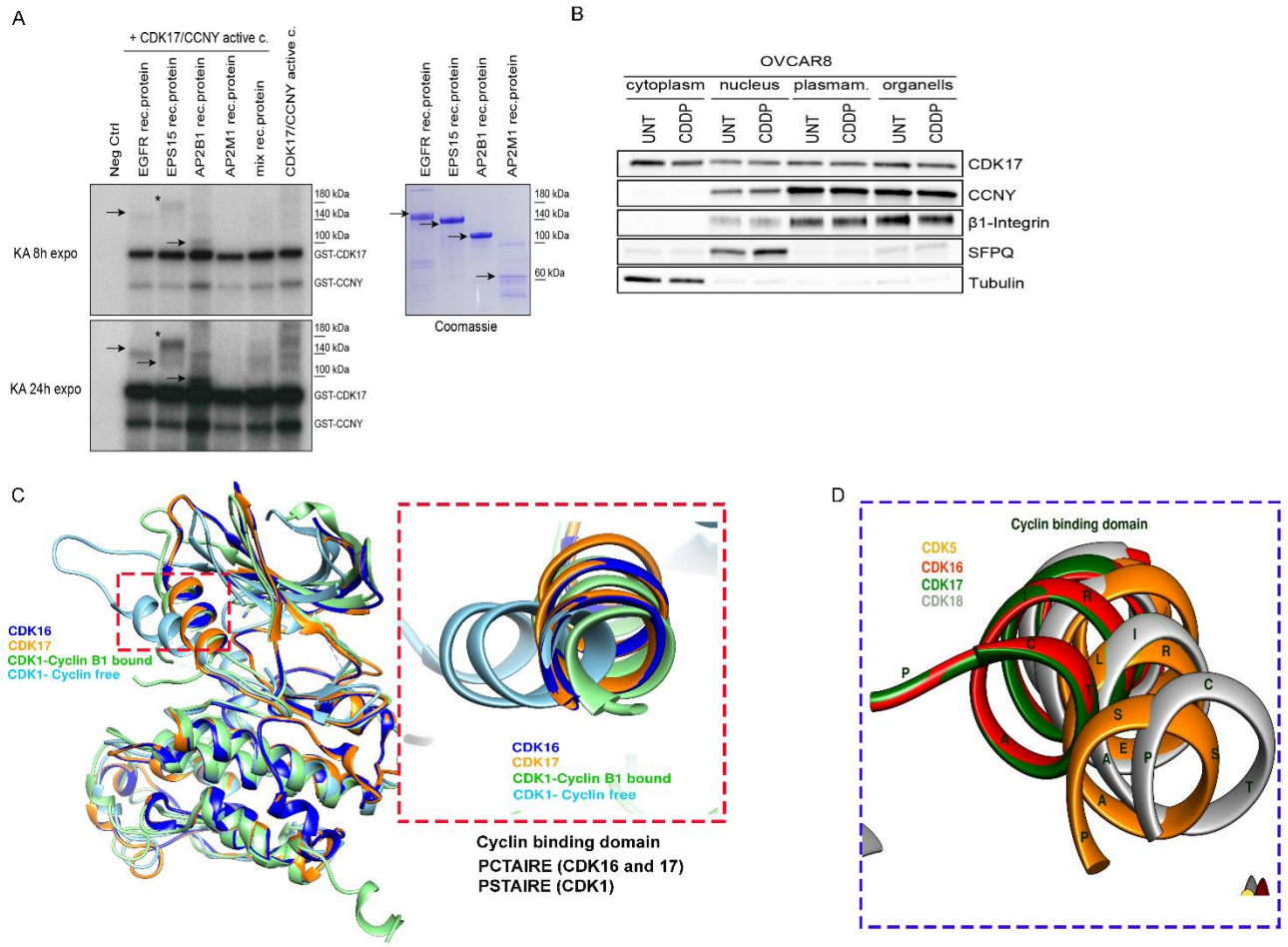

Figure 4.12 3D CDK17 configuration support the possibility that it has cyclin-free activity A) In vitro kinase assays were performed incubating 500 ng of recombinant CDK17-CCNY active complex with 2 µg of EGFR, EPS15, AP2B1, AP2M1 recombinant proteins as substrates. Arrows indicate respective bands for each protein, and the asterisks depict

hyperphosphorylated EPS15 band**.** On the right coomasie staining of the corresponding recombinant proteins used. **B)** WB depicting cellular localization of CDK17 and CCNY proteins. Tubulin, SFPQ and β1-integrin were used as normalizer for specific compartments, cytosplasm, nucleus and plasma membrane/organelles respectively. **C**)Homology modelled-CDK17 and CDK16 [PDB 5G6V] structures were superimposed with CDK1[PDB 4YC6] cyclin-free and CDK1[PDB 4YC3] cyclin-bound proteins. In the box zoom-in view of the cyclin-binding domains is shown. **D)** Homology model was generated for CDK18 using CDK16[PDB 56GV] as template and then CDK16-18 were superimposed with CDK5[PDB 1H4L]structure.

4.10 CDK17 silencing sensitizes EOC cell lines to EGFR blockage

Given its essential roles in several biological processes, EGFR has been one of the most promising targets for cancer treatment and several approved drugs are clinically available. For instance, EGFR inhibitors, like Gefitinib, Erlotinib have been proven to be efficient in settings of EGFR-addicted cancers, such as non-small cell lung cancer, where activation mutation of EGFR is frequent.[107] Even if EGFR role in EOC settings is poorly investigated, previous results using non-conventional staining in a cohort of 150 advanced EOC patients, identified high EGFR expression as the most significant prognostic factor for both shorter disease-free and overall survival.[108]

To understand if the modulation of CDK17 expression would have any impact in EOC cells to respond to EGFR blockage, we treated MDAH and OVCAR8 cells, silenced for CDK17 or not, with Gefitinib, an ATP-competitive EGFR inhibitor. Results showed that silencing of CDK17 significantly reduces cell viability under Gefitinib treatment (Figure 4.13A). These results were then confirmed in kill curve analyses demonstrating that CDK17 silencing reduces Gefitinib IC50 by the half in OVCAR8 cells (Figure 4.13B). More importantly, we also observed that CDK17 silencing improved Gefitinib efficacy in the context of PT-resistant cells (Figure 4.13C). Moreover, combining CDDP and Gefitinib treatments in PT-Resistant OVCAR8 cells, we showed that sequential usage of CDDP and Gefitinib further potentiates cytotoxicity of CDDP treatment alone (Figure 4.13D).

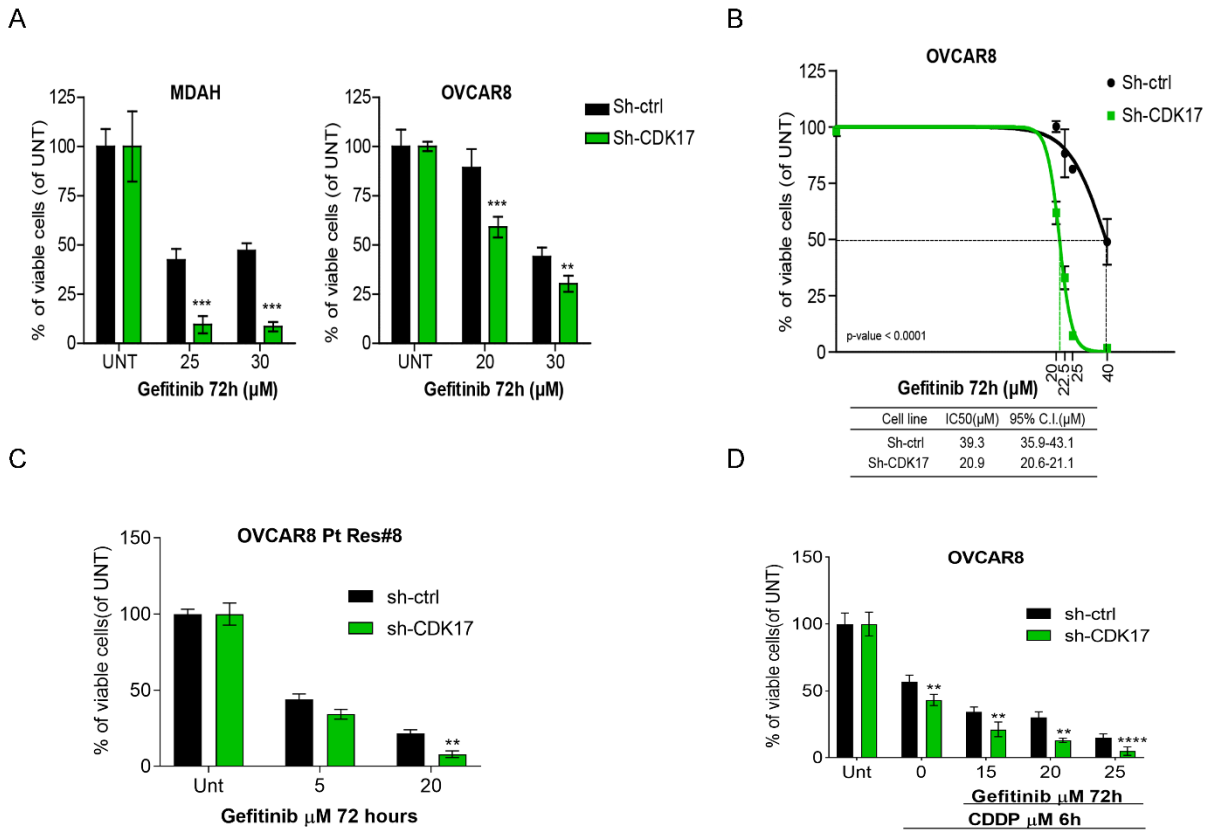

Figure 4.13 CDK17 silencing sensitizes EOC cells to Gefitinib. A) Dose-response curve of MDAH and OVCAR8 transduced with Sh-ctrl and Sh-CDK17 treated with increasing doses of Gefitinib for 72h. Data are expressed as percentage of viable cells respect to untreated cells and represent the mean (± SD) of 3 biological replicates. Statistical significance was determined by a two-tailed, unpaired Student's t-test (**p<0.01, ***p<0.001). **B**) Nonlinear regression analyses of cell viability in OVCAR8 cells, transduced with Sh-ctrl and Sh-CDK17, treated with increasing doses of Gefitinib for 72 hours. The table shows the IC50 and the confidence interval (CI) of each condition. Data are expressed as percentage of viable cells respect to untreated cells and represent the mean (± SD) of 3 biological replicates. Fisher's exact test was used to calculate the global p-value reported in the graph. **C**) Dose-response curve of OVCAR8 Pt Res#8 Sh-ctrl and Sh-CDK17 cells treated with increasing doses of Gefitinib for 72h. Data are expressed as percentage of viable cells respect to untreated cells and represent the mean (± SD) of 3 biological replicates. Statistical significance was determined by a two-tailed, unpaired Student's t-test (**p<0.01, ***p<0.001). **D)** OVCAR8 Sh-ctrl and Sh-CDK17 cells treated with a fixed dose of CDDP (15μM) for 6h and then released with increasing doses of Gefitinib for a total time course of 72h. Data are expressed as percentage of viable cells respect to untreated cells and represent the mean (± SD) of 3 biological replicates. Statistical significance was determined by a two-tailed, unpaired Student's t-test (**p<0.01, ***p<0.001).

5. Discussion

In HGEOC patients' response to Platinum (PT)-based chemotherapy dictates subsequent treatments and predicts prognosis. Despite initial effectiveness most patients develop resistance to PT-compounds. To overcome the onset of PT-resistance, in the past few decades, the mainstream research direction investigated if the combination between targeted therapies and standard chemotherapy, could improve the disease-free survival of selected group of patients. In this regard, combining PARP inhibition with chemotherapy demonstrated significant benefits in patients carrying germline or somatic BRCA1/2 gene mutations or deficient in the Homologous Recombination DNA repair pathway. These findings open the way to consider combination therapies as a valid approach in EOC management to prevent and/or overcome the emergence of PT-resistance. Therefore, there is an urgent need for comprehensive understanding of the underlying mechanisms and molecular alterations that could explain the onset of PT-resistance and eventually find new actionable targets to translate into clinics. It has been already demonstrated that the employment of high-throughput screenings, such as synthetic lethal high-throughput RNAi screens, is an invaluable tool to identify new potential and highly selective therapeutic targets, whose silencing may synergise with chemotherapy to potentiate cell death and possibly overcome resistance. In this light the involvement of Cyclin Dependent Kinases (CDKs), in several biological processes like cell cycle, transcription, translation, and mRNA processing and/or DNA damage response depict these kinases as an attractive target to decipher carcinogenesis and chemo-resistance. Starting from an unbiased loss of function shRNA screening, targeting all 23 human CDKs we recently identified CDK6 and CDK17 as possibly involved in the response to platinum in EOC cells.

In this PhD Thesis project, we have dissected the role of CDK17 (PCTAIRE2), a member of the largely unexplored CDKs subfamily PCTAIRE. PCTAIREs subfamily is composed by CDK16, CDK17 and CDK18 and very little information are available about their functional roles and their possible implications in cancer. Only few recent studies, mainly regarding the role of CDK16 and CDK18 in cell proliferation, or anti-apoptotic function in different type of malignancies, started shedding light on their possible function in these processes. Among PCTAIRE family members CDK17 is the least studied and here we have reported for the first time a possible role for CDK17 in EOC response to PT. Our data strongly indicated that CDK17 is involved in the regulation of endocytosis in EOC likely through the control of EGFR pathway, shedding new light on the regulation of a hub signalling oncogenic pathway with potential clinical translation.

We have demonstrated that silencing of CDK17 significantly increased PT-induced cell death in different EOCs models and that, vice versa, of CDK17 overexpression conferred an increased resistance to PT. Using clinically relevant CDK17 mutant proteins carrying missense mutations

identified in HGEOC samples (R312G and K343N) we demonstrated that these mutations are particularly active in protecting EOC from PT-induced death. It will be worth studying if the pressure of PT could induce the appearance of CDK17 mutation in HGEOC. The analyses of the COSMIC database[91] reporting the mutations found in all human cancers, showed that CDK17 is most frequently mutated in endometrial carcinomas, which share with ovarian cancer several molecular alterations. We have, therefore, already planned to deeply sequence PT-resistant in vitro models and human samples, with an NGS custom panel able to define the frequency of CDKs mutation in this particular clinical condition.

It is worth noting that, both mutations identified in HGEOC are located in CDK17 kinase domain and particularly, R312G mutation is mapped to the HRD domain, that is indispensable for the proper activation of CDKs. At this regard it will be important to define if these mutations are associated with different kinase activity and/or with a different cyclin independent activation. In silico 3D conformation analyses and in vitro studies are in progress to clarify this point. Indeed, it has been postulated that without activating partners (canonically the cyclins) CDKs are monomeric and inactive. Nothing it is known about the activating partner of CDK17 that is the least studied member of all CDKs. Yet, its closest homologs CDK16 and CDK18 have been shown to interact with cyclin Y and cyclin A2. Our initial co-IP experiments looking at the interaction of CDK17 with several cyclins were unsuccessful in confirming its interaction with any of the studied partners (not shown in this thesis). Similarly, an unbiased proteomic approach used to define the CDK17 interactome in EOC cells did not retrieve any a classical cyclin as CDK17 binding partner in EOC cells. Several explanations could arise from these observations including the possible weakness of CDK17- cyclin Y interaction or a particular subcellular localization of the two proteins. At this regard we have showed that in our model cyclin Y is almost absent in cytoplasm and it could interact with CDK17 only in the membrane or nuclear compartments where both proteins are expressed.

Also, our in -silico analysis revealed that CDK17 cyclin binding domain is very similar to that of CDK16 and well overlaps with the 3D-configuration of the active cyclin-bound domain of CDK1. These observations could allow us to preliminarily speculate that CDK17 (and also CDK16) could have a cyclin independent kinase activity. We, also compared CDK16 and CDK17 structure with that archetypical non-canonical CDKs, CDK5, and with the other member of PCTAIRE family CDK18. This analysis demonstrated that the topological overlap between the cyclin binding domains of CDK16, CDK17 and active CDK1, were not shared with CDK5 and CDK18, but are specific for CDK16 and CDK17. It would be extremely useful to further compare the cyclin binding domains of CDK16 and CDK17 with the one of PFTAIRE proteins (CDK14 and CDK15) to see if they share

common 3D features. On the other side we are aware that cyclin binding to CDKs is also considered necessary to confer the kinase with substrate specificity. It is therefore important to understand how CDK17 (and possibly CDK16) define their interactors in the absence of a proper cyclin as binding and activating partner. At this regard it is worth to mention that cyclin-box like motifs could be contained also in proteins not classified as cyclins that could activate non-canonical CDKs. This is for instance the case of CDK5 whose binding partners could be p35, its splicing product p25 or Cables, all not classified as cyclins.[109] Preliminary in silico analyses we performed to map the cyclin-box sequence in proteins retrieved by mass spectrometry analysis as CDK17 binding partners revealed that several of them contained a cyclin or cyclin-like box. Among the others, BASP1 protein seems a promising candidate, being one of the most enriched proteins. We will experimentally evaluate in future experiments if BASP1 could act as CDK17 activating partner.

The results from Mass Spectrometry analyses and co-IP experiments clearly demonstrated that in our EOC models CDK17 binds to several proteins belonging to EGFR and vesicular trafficking pathways. Here it's worth to note that two proteins from the list of most enriched proteins (AP2A2 and EPS15) have already been documented to dictate the fate of internalized EGFR, further supporting the hypothesis that CDK17 is involved in the regulation of EGFR activity.[93] Collectively, our experiments showed that the presence of CDK17 could maintain over the time higher phosphorylation levels of ligand stimulated EGFR, localized into vesicle compartments. Endocytosis is essential for cell homeostasis and its dysregulation has been linked to different aspects of tumorigenesis, such as dysregulated membrane receptor signalling, adhesion, dissemination and loss of epithelial cell polarity. [110–112] Interestingly stress induced EGFR activation, including platinum treatment, protect the cells from apoptosis and relies on EGFR signalling from endosome.[101] These evidences are in line with our results demonstrating that CDK17 is necessary to sustain stress induced EGFR activity and that it protects EOC cells from PT-induced death. Whether these two activities of CDK17 are linked and if EGFR is a key mediator of CDK17-mediated cell survival upon PT treatment is something currently under investigation.

We have also demonstrated that CDDP does not have any impact on EGFR phosphorylation on Threonine 669 reported in literature as stress-induced phosphorylation.[113] However, by generic pThr/pSer IP we were able to show that, under CDDP-exposure, CDK17 presence leads to Threonine phosphorylation of EGFR protein. Accordingly, *in vitro* kinase assay demonstrated that CDK17-CCNY active complex readily phosphorylates not only EGFR, but also subunit of AP2B1 protein of AP2 complex and possibly EPS15.

It is known that under stress conditions, when EGFR is bound by both AP2A2 and EPS15, is protected from degradation, on the contrary when only EPS15 is bound to EGFR, leads to its degradation.[93] Our immunoprecipitation data shows that CDK17 promotes interaction between AP2A2 and EPS15 and by doing so, CDK17 may protect EGFR from degradation. In future studies we will try to understand if CDK17 silencing abrogates the interaction between EGFR and AP2 complex, trying to dissect if this process is phosphorylation dependent or not. If this will be the case, we can propose CDK17 inhibitors, now under development,[114] as new possible therapeutic agents able to impair EGFR anti-apoptotic role upon platinum in EOC and possibly other type of cancers in which EGFR represents a validated therapeutic target like lung, head and neck and colon cancers.

Although EGFR is overexpressed or mutated in several human cancers in EOC its hasn't been thoroughly studied. Previous literature results suggested that it was linked to PT-resistance and worse prognosis, yet in the TCGA-HGSOC dataset EGFR was neither frequently mutated or overexpressed[10] and clinical trials evaluating the efficacy of EGFR inhibition as single agent in PT-resistant EOC patients failed to meet the expectations.[115,116] These data could suggest that EGFR per se is not a good biomarker to select patients that might benefit from anti EGFR therapy. It is however possible that the identification of appropriate biomarkers could define a subpopulation of EOC patients, who may benefit from EGFR targeted therapies used alone or in combination with other agents. We have shown that CDK17 silencing is able to sensitize both parental cells and PT-resistant cells to the EGFR inhibitor Gefitinib. Moreover, combining CDDP and Gefitinib treatments in PT-Resistant OVCAR8 cells, we showed that sequential usage of CDDP and Gefitinib further potentiates cytotoxicity of CDDP treatment alone. These results, along with the observation that PT-resistant cells had higher levels of CDK17 protein might have translational relevance supporting the hypothesis that CDK17 could represent a predictive biomarker of anti-EGFR therapies. This possibility needs to be fully investigated in human samples and appropriate in vivo models.

Overall, in thesis work we have identified a new and unexpected role for CDK17 in the control of PT-induced death and EGFR signaling. To our knowledge this is the first observation that a CDK could bind to and regulate the recycling of EGFR. Even if more work is necessary to properly characterize this new pathway and its relevance to the human pathology, we believe that our results have contributed to characterize a new mechanism that in EOC could lead to platinum resistance that will potentially result in the definition of new therapeutic options for PT-resistant EOC patients that still do not have clinically effective treatments.

6. References

1. Cabasag, C. J. *et al.* The influence of birth cohort and calendar period on global trends in ovarian cancer incidence. *Int. J. cancer* **146**, 749–758 (2020).

2. Ferlay, J. *et al.* Estimating the global cancer incidence and mortality in 2018: GLOBOCAN sources and methods. *Int. J. cancer* **144**, 1941–1953 (2019).

3. Zhang, K. *et al.* Cross-validation of genes potentially associated with neoadjuvant chemotherapy and platinum-based chemoresistance in epithelial ovarian carcinoma. *Oncol. Rep.* **44**, 909–926 (2020).

4. van Zyl, B., Tang, D. & Bowden, N. A. Biomarkers of platinum resistance in ovarian cancer: what can we use to improve treatment. *Endocr. Relat. Cancer* **25**, R303–R318 (2018).

5. Stewart, C., Ralyea, C. & Lockwood, S. Ovarian Cancer: An Integrated Review. *Semin. Oncol. Nurs.* **35**, 151–156 (2019).

6. Karnezis, A. N., Cho, K. R., Gilks, C. B., Pearce, C. L. & Huntsman, D. G. The disparate origins of ovarian cancers: pathogenesis and prevention strategies. *Nat. Rev. Cancer* **17**, 65–74 (2017).

7. Javadi, S., Ganeshan, D. M., Qayyum, A., Iyer, R. B. & Bhosale, P. Ovarian Cancer, the Revised FIGO Staging System, and the Role of Imaging. *AJR. Am. J. Roentgenol.* **206**, 1351–1360 (2016).

8. Ramalingam, P. Morphologic, Immunophenotypic, and Molecular Features of Epithelial Ovarian Cancer. *Oncology (Williston Park).* **30**, 166–176 (2016).

9. Shih, I. M. & Kurman, R. J. Ovarian Tumorigenesis: A Proposed Model Based on Morphological and Molecular Genetic Analysis. *Am. J. Pathol.* **164**, 1511–1518 (2004).

10. Bell, D. *et al.* Integrated genomic analyses of ovarian carcinoma. *Nature* **474**, 609–615 (2011).

11. Testa, U., Petrucci, E., Pasquini, L., Castelli, G. & Pelosi, E. Ovarian Cancers: Genetic Abnormalities, Tumor Heterogeneity and Progression, Clonal Evolution and Cancer Stem Cells. *Medicines* **5**, 16 (2018).

12. Jones, P. M. & Drapkin, R. Modeling High-Grade Serous Carcinoma: How Converging Insights into Pathogenesis and Genetics are Driving Better Experimental Platforms. *Front. Oncol.* **3**, 217 (2013).

13. Colombo, N. *et al.* ESMO-ESGO consensus conference recommendations on ovarian cancer: pathology and molecular biology, early and advanced stages, borderline tumours and recurrent disease†. *Ann. Oncol. Off. J. Eur. Soc. Med. Oncol.* **30**, 672–705 (2019).

14. Horwitz, S. B. Taxol (paclitaxel): mechanisms of action. *Ann. Oncol. Off. J. Eur. Soc. Med. Oncol.* **5 Suppl 6**, S3-6 (1994).

15. Cooke, S. L. & Brenton, J. D. Evolution of platinum resistance in high-grade serous ovarian cancer. *Lancet. Oncol.* **12**, 1169–1174 (2011).

16. Rocha, C. R. R., Silva, M. M., Quinet, A., Cabral-Neto, J. B. & Menck, C. F. M. DNA repair pathways and cisplatin resistance: an intimate relationship. *Clinics (Sao Paulo).* **73**, e478s (2018).

17. Lheureux, S., Gourley, C., Vergote, I. & Oza, A. M. Epithelial ovarian cancer. *Lancet (London, England)* **393**, 1240–1253 (2019).

18. Matulonis, U. A. *et al.* Ovarian cancer. *Nat. Rev. Dis. Prim.* **2**, 16061 (2016).

19. Oronsky, B. *et al.* A brief review of the management of platinum-resistant-platinum-refractory ovarian cancer. *Med. Oncol.* **34**, 103 (2017).

20. Freimund, A. E., Beach, J. A., Christie, E. L. & Bowtell, D. D. L. Mechanisms of Drug Resistance in High-Grade Serous Ovarian Cancer. *Hematol. Oncol. Clin. North Am.* **32**, 983–996 (2018).

21. Konstantinopoulos, P. A. & Matulonis, U. A. Targeting DNA Damage Response and Repair as a Therapeutic Strategy for Ovarian Cancer. *Hematol. Oncol. Clin. North Am.* **32**, 997–1010 (2018).

22. Ledermann, J. A. PARP inhibitors in ovarian cancer. *Ann. Oncol.* **27**, i40–i44 (2016).

23. Dias, M. P., Moser, S. C., Ganesan, S. & Jonkers, J. Understanding and overcoming resistance to PARP inhibitors in cancer therapy. *Nat. Rev. Clin. Oncol.* (2021) doi:10.1038/s41571-021-00532-x.

24. Boussios, S. *et al.* Combined Strategies with Poly (ADP-Ribose) Polymerase (PARP) Inhibitors for the Treatment of Ovarian Cancer: A Literature Review. *Diagnostics (Basel, Switzerland)* **9**, (2019).

25. Jiao, S. *et al.* PARP Inhibitor Upregulates PD-L1 Expression and Enhances Cancer-Associated Immunosuppression. *Clin. cancer Res. an Off. J. Am. Assoc. Cancer Res.* **23**, 3711–3720 (2017).

26. Konstantinopoulos, P. A. *et al.* Single-Arm Phases 1 and 2 Trial of Niraparib in Combination With Pembrolizumab in Patients With Recurrent Platinum-Resistant Ovarian Carcinoma. *JAMA Oncol.* **5**, 1141–1149 (2019).

27. Lapenna, S. & Giordano, A. Cell cycle kinases as therapeutic targets for cancer. *Nat. Rev. Drug Discov.* **8**, 547–566 (2009).

28. Dall'Acqua, A. *et al.* Inhibition of CDK4/6 as Therapeutic Approach for Ovarian Cancer Patients: Current Evidences and Future Perspectives. *Cancers (Basel).* **13**, (2021).

29. Dean, J. L., McClendon, A. K. & Knudsen, E. S. Modification of the DNA damage response by therapeutic CDK4/6 inhibition. *J. Biol. Chem.* **287**, 29075–29087 (2012).

30. Dall'Acqua, A. *et al.* CDK6 protects epithelial ovarian cancer from platinum-induced death via FOXO3 regulation. *EMBO Mol. Med.* **9**, 1415–1433 (2017).

31. Goel, S. *et al.* CDK4/6 inhibition triggers anti-tumour immunity. *Nature* **548**, 471–475 (2017).

32. Cole, A. J. *et al.* Assessing mutant p53 in primary high-grade serous ovarian cancer using immunohistochemistry and massively parallel sequencing. *Sci. Rep.* **6**, 26191 (2016).

33. Chen, S.-H. & Chang, J.-Y. New Insights into Mechanisms of Cisplatin Resistance: From Tumor Cell to Microenvironment. *Int. J. Mol. Sci.* **20**, 4136 (2019).

34. Varjosalo, M. *et al.* The Protein Interaction Landscape of the Human CMGC Kinase Group. *Cell Rep.* **3**, 1306–1320 (2013).

35. Per Hydbring1, 2, Marcos Malumbres3, and Piotr Sicinski1, 2 1Department. Non-canonical functions of cell cycle cyclins and cyclin- dependent kinases. *Nat Rev Mol Cell Biol.* **176**, 280–292 (2016).

36. Malumbres, M. Cyclin-dependent kinases. *Genome Biol.* **15**, 122 (2014).

37. Satyanarayana, A. & Kaldis, P. Mammalian cell-cycle regulation: several Cdks, numerous cyclins and diverse compensatory mechanisms. *Oncogene* **28**, 2925–2939 (2009).

38. Tian, B., Yang, Q. & Mao, Z. Phosphorylation of ATM by Cdk5 mediates DNA damage signalling and regulates neuronal death. *Nat. Cell Biol.* **11**, 211–218 (2009).

39. Barone, G. *et al.* Human CDK18 promotes replication stress signaling and genome stability. **44**, 8772–8785 (2016).

40. Mikolcevic, P., Rainer, J. & Geley, S. Orphan kinases turn eccentric: a new class of cyclin Y-activated, membrane-targeted CDKs. *Cell Cycle* **11**, 3758–3768 (2012).

41. Kaldis, P., Cheng, A. & Solomon, M. J. The effects of changing the site of activating phosphorylation in CDK2 from threonine to serine. *J. Biol. Chem.* **275**, 32578–32584 (2000).

42. Dixon-Clarke, S. E. *et al.* Structure and inhibitor specificity of the PCTAIRE-family kinase CDK16. *Biochem. J.* **474**, 699–713 (2017).

43. Besset, V., Rhee, K. & Wolgemuth, D. J. The cellular distribution and kinase activity of the Cdk family member Pctaire 1 in the adult mouse brain and testis suggest functions in differentiation. *Cell Growth Differ.* **10**, 173–181 (1999).

44. Le Bouffant, F., Capdevielle, J., Guillemot, J. C. & Sladeczek, F. Characterization of brain PCTAIRE-1 kinase immunoreactivity and its interactions with p11 and 14-3-3 proteins. *Eur. J. Biochem.* **257**, 112–120 (1998).

45. Hirose, T., Tamaru, T., I, N. O., Nagai, K. & Okada, M. PCTAIRE 2 , a Cdc2-related serinehhreonine kinase , is predominantly expressed in terminally differentiated neurons. **488**, 481–488 (1997).

46. Hirose, T. *et al.* Identification of tudor repeat associator with PCTAIRE 2 (Trap). A novel protein that interacts with the N-terminal domain of PCTAIRE 2 in rat brain. *Eur. J. Biochem.* **267**, 2113–2121 (2000).

47. Mikolcevic, P. *et al.* Cyclin-Dependent Kinase 16/PCTAIRE Kinase 1 Is Activated by Cyclin Y and Is Essential for Spermatogenesis. *Mol. Cell. Biol.* **32**, 868–879 (2012).

48. Shehata, S. N. *et al.* Cyclin Y phosphorylation- and 14-3-3-binding-dependent activation of PCTAIRE-1/CDK16. *Biochem. J.* **469**, 409–420 (2015).

49. Dohmen, M. *et al.* AMPK-dependent activation of the Cyclin Y/CDK16 complex controls autophagy. *Nat. Commun.* **11**, 1032 (2020).

50. Zi, Z. *et al.* CCNYL1, but Not CCNY, Cooperates with CDK16 to Regulate Spermatogenesis in Mouse. *PLoS Genet.* **11**, 1–22 (2015).

51. Matsuda, S. *et al.* PCTAIRE Kinase 3 / Cyclin-dependent Kinase 18 Is Activated through Association with Cyclin A and / or Phosphorylation by Protein Kinase A *. **289**, 18387–18400 (2014).

52. Graeser, R. *et al.* Regulation of the CDK-related protein kinase PCTAIRE-1 and its possible

role in neurite outgrowth in Neuro-2A cells. *J. Cell Sci.* **115**, 3479–3490 (2002).

53. Mokalled, M. H., Johnson, A., Kim, Y., Oh, J. & Olson, E. N. Myocardin-related transcription factors regulate the Cdk5/Pctaire1 kinase cascade to control neurite outgrowth, neuronal migration and brain development. *Development* **137**, 2365–2374 (2010).

54. Pedersen, A.-K. *et al.* Proteomic investigation of Cbl and Cbl-b in neuroblastoma cell differentiation highlights roles for SHP-2 and CDK16. *iScience* **24**, 102321 (2021).

55. Pan, Y. *et al.* Cyclin-dependent Kinase 18 Promotes Oligodendrocyte Precursor Cell Differentiation through Activating the Extracellular Signal-Regulated Kinase Signaling Pathway. *Neurosci. Bull.* **35**, 802–814 (2019).

56. Palmer, K. J., Konkel, J. E. & Stephens, D. J. PCTAIRE protein kinases interact directly with the COPII complex and modulate secretory cargo transport. *J. Cell Sci.* **118**, 3839 LP – 3847 (2005).

57. Pozuelo Rubio, M. *et al.* 14-3-3-affinity purification of over 200 human phosphoproteins reveals new links to regulation of cellular metabolism, proliferation and trafficking. *Biochem. J.* **379**, 395–408 (2004).

58. O'Kelly, I., Butler, M. H., Zilberberg, N. & Goldstein, S. A. N. Forward transport. 14-3-3 binding overcomes retention in endoplasmic reticulum by dibasic signals. *Cell* **111**, 577–588 (2002).

59. Wu, K. *et al.* Enhanced expression of Pctk1, Tcf12 and Ccnd1 in hippocampus of rats: Impact on cognitive function, synaptic plasticity and pathology. *Neurobiol. Learn. Mem.* **97**, 69–80 (2012).

60. Khawaja, X., Xu, J., Liang, J. J. & Barrett, J. E. Proteomic Analysis of Protein Changes Developing in Rat Hippocampus after Chronic Antidepressant Treatment: Implications for Depressive Disorders and Future Therapies. *J. Neurosci. Res.* **75**, 451–460 (2004).

61. Iancu, O. D. *et al.* On the relationships in rhesus macaques between chronic ethanol consumption and the brain transcriptome. *Addict. Biol.* **23**, 196–205 (2018).

62. Herskovits, A. Z. & Davies, P. The regulation of tau phosphorylation by PCTAIRE 3: Implications for the pathogenesis of Alzheimer's disease. *Neurobiol. Dis.* **23**, 398–408 (2006).

63. Chaput, D., Kirouac, L., Stevens Jr, S. M. & Padmanabhan, J. Potential role of PCTAIRE-2, PCTAIRE-3 and P-Histone H4 in amyloid precursor protein-dependent Alzheimer pathology. *Oncotarget* **7**, 8481–8497 (2016).

64. Xie, J. *et al.* CDK16 phosphorylates and degrades p53 to promote radioresistance and predicts prognosis in lung cancer. *Theranostics* **8**, 650–662 (2018).

65. Hernández-Ortega, S. *et al.* Phosphoregulation of the oncogenic protein regulator of cytokinesis 1 (PRC1) by the atypical CDK16/CCNY complex. *Exp. Mol. Med.* **51**, 1–17 (2019).

66. Garwain, O., Valla, K. & Scarlata, S. Phospholipase Cβ1 regulates proliferation of neuronal cells. *FASEB J.* **32**, 2891–2898 (2018).

67. Phadke, M. *et al.* Dabrafenib inhibits the growth of BRAF-WT cancers through CDK16 and NEK9 inhibition. *Mol. Oncol.* **12**, 74–88 (2018).

68. Naumann, U. *et al.* PCTAIRE3: A putative mediator of growth arrest and death induced by

CTS-1, a dominant-positive p53-derived synthetic tumor suppressor, in human malignant glioma cells. *Cancer Gene Ther.* **13**, 469–478 (2006).

69. Leonardi, M., Perna, E., Tronnolone, S., Colecchia, D. & Chiariello, M. Activated kinase screening identifies the IKBKE oncogene as a positive regulator of autophagy. *Autophagy* **15**, 312–326 (2019).

70. Yanagi, T., Shi, R., Aza-Blanc, P., Reed, J. C. & Matsuzawa, S. I. PCTAIRE1-Knockdown sensitizes cancer cells to TNF family cytokines. *PLoS One* **10**, 1–19 (2015).

71. Ning, J. F. *et al.* Myc targeted CDK18 promotes ATR and homologous recombination to mediate PARP inhibitor resistance in glioblastoma. *Nat. Commun.* **10**, (2019).

72. Matsuda, S., Kawamoto, K., Miyamoto, K., Tsuji, A. & Yuasa, K. PCTK3/CDK18 regulates cell migration and adhesion by negatively modulating FAK activity. *Sci. Rep.* **7**, 1–15 (2017).

73. Hussain Qureshi, M. F. *et al.* Gene signatures of cyclin-dependent kinases: a comparative study in naïve early and advanced stages of lung metastasis breast cancer among pre- and post-menopausal women. *Genes Cancer* **12**, 1–11 (2021).

74. Bai, J. *et al.* A high-throughput screen for genes essential for PRRSV infection using a piggyBac-based system. *Virology* **531**, 19–30 (2019).

75. Liu, M. *et al.* The Identification of Key Genes and Pathways in Glioma by Bioinformatics Analysis. *J. Immunol. Res.* **2017**, 1278081 (2017).

76. Demirkan, A. *et al.* Genome-wide association study identifies novel loci associated with circulating phospho- and sphingolipid concentrations. *PLoS Genet.* **8**, e1002490–e1002490 (2012).

77. Sonego, M. *et al.* Common biological phenotypes characterize the acquisition of platinum-resistance in epithelial ovarian cancer cells. *Sci. Rep.* **7**, 7104 (2017).

78. Sonego, M. *et al.* Stathmin regulates mutant p53 stability and transcriptional activity in ovarian cancer. *EMBO Mol. Med.* **5**, 707–722 (2013).

79. Casabona, M. G., Vandenbrouck, Y., Attree, I. & Couté, Y. Proteomic characterization of Pseudomonas aeruginosa PAO1 inner membrane. *Proteomics* **13**, 2419–2423 (2013).

80. Bouyssié, D. *et al.* Proline: an efficient and user-friendly software suite for large-scale proteomics. *Bioinformatics* **36**, 3148–3155 (2020).

81. Couté, Y., Bruley, C. & Burger, T. Beyond Target-Decoy Competition: Stable Validation of Peptide and Protein Identifications in Mass Spectrometry-Based Discovery Proteomics. *Anal. Chem.* **92**, 14898–14906 (2020).

82. Wieczorek, S. *et al.* DAPAR & ProStaR: software to perform statistical analyses in quantitative discovery proteomics. *Bioinformatics* **33**, 135–136 (2017).

83. Schindelin, J. *et al.* Fiji: an open-source platform for biological-image analysis. *Nat. Methods* **9**, 676–682 (2012).

84. Paul Shannon, 1 *et al.* Cytoscape: A Software Environment for Integrated Models. *Genome Res.* **13**, 426 (1971).

85. Bader, G. D. & Hogue, C. W. V. An automated method for finding molecular complexes in large protein interaction networks. *BMC Bioinformatics* **4**, 2 (2003).

86. Ghandi, M. *et al.* Next-generation characterization of the Cancer Cell Line Encyclopedia. *Nature* **569**, 503–508 (2019).

87. Gu, Z., Eils, R. & Schlesner, M. Complex heatmaps reveal patterns and correlations in multidimensional genomic data. *Bioinformatics* **32**, 2847–2849 (2016).

88. Webb, B. & Sali, A. Comparative Protein Structure Modeling Using MODELLER. *Curr. Protoc. Bioinforma.* **54**, 5.6.1-5.6.37 (2016).

89. Meng, E. C., Pettersen, E. F., Couch, G. S., Huang, C. C. & Ferrin, T. E. Tools for integrated sequence-structure analysis with UCSF Chimera. *BMC Bioinformatics* **7**, 1–10 (2006).

90. Mosesson, Y., Mills, G. B. & Yarden, Y. Derailed endocytosis: an emerging feature of cancer. *Nat. Rev. Cancer* **8**, 835–850 (2008).

91. Tate, J. G. *et al.* COSMIC: the Catalogue Of Somatic Mutations In Cancer. *Nucleic Acids Res.* **47**, D941–D947 (2019).

92. Tan, X., Lambert, P. F., Rapraeger, A. C. & Anderson, R. A. Stress-Induced EGFR Trafficking: Mechanisms, Functions, and Therapeutic Implications. *Trends Cell Biol.* **26**, 352–366 (2016).

93. Pascolutti, R. *et al.* Molecularly Distinct Clathrin-Coated Pits Differentially Impact EGFR Fate and Signaling. *Cell Rep.* **27**, 3049-3061.e6 (2019).

94. Stark, C. *et al.* BioGRID: a general repository for interaction datasets. *Nucleic Acids Res.* **34**, D535-9 (2006).

95. Barretina, J. *et al.* The Cancer Cell Line Encyclopedia enables predictive modelling of anticancer drug sensitivity. *Nature* **483**, 603–607 (2012).

96. Sorkina, T., Bild, A., Tebar, F. & Sorkin, A. Clathrin, adaptors and eps15 in endosomes containing activated epidermal growth factor receptors. *J. Cell Sci.* **112 (Pt 3**, 317–327 (1999).

97. Bishop, N., Horman, A. & Woodman, P. Mammalian class E vps proteins recognize ubiquitin and act in the removal of endosomal protein–ubiquitin conjugates . *J. Cell Biol.* **157**, 91–102 (2002).

98. Malerød, L., Stuffers, S., Brech, A. & Stenmark, H. Vps22/EAP30 in ESCRT-II Mediates Endosomal Sorting of Growth Factor and Chemokine Receptors Destined for Lysosomal Degradation. *Traffic* **8**, 1617–1629 (2007).

99. Bache, K. G. *et al.* The ESCRT-III Subunit hVps24 Is Required for Degradation but Not Silencing of the Epidermal Growth Factor Receptor. *Mol. Biol. Cell* **17**, 2513–2523 (2006).

100. Tanaka, T., Ozawa, T., Oga, E., Muraguchi, A. & Sakurai, H. Cisplatin-induced non-canonical endocytosis of EGFR via p38 phosphorylation of the C-terminal region containing Ser-1015 in non-small cell lung cancer cells. *Oncol. Lett.* **15**, 9251–9256 (2018).

101. Tomas, A. *et al.* WASH and Tsg101/ALIX-dependent diversion of stress-internalized EGFR from the canonical endocytic pathway. *Nat. Commun.* **6**, 7324 (2015).

102. Granados, M. L., Hudson, L. G. & Samudio-Ruiz, S. L. Contributions of the Epidermal Growth Factor Receptor to Acquisition of Platinum Resistance in Ovarian Cancer Cells. *PLoS One* **10**, e0136893 (2015).

103. Zwang, Y. & Yarden, Y. p38 MAP kinase mediates stress-induced internalization of EGFR:

implications for cancer chemotherapy. *EMBO J.* **25**, 4195–4206 (2006).

104. Refaat, A. *et al.* Role of tyrosine kinase-independent phosphorylation of EGFR with activating mutation in cisplatin-treated lung cancer cells. *Biochem. Biophys. Res. Commun.* **458**, 856–861 (2015).

105. Sunada, H., Magun, B. E., Mendelsohn, J. & MacLeod, C. L. Monoclonal antibody against epidermal growth factor receptor is internalized without stimulating receptor phosphorylation. *Proc. Natl. Acad. Sci. U. S. A.* **83**, 3825–3829 (1986).

106. Pozzi, C. *et al.* The EGFR-specific antibody cetuximab combined with chemotherapy triggers immunogenic cell death. *Nat. Med.* **22**, 624–631 (2016).

107. Kris, M. G. *et al.* Efficacy of Gefitinib, an Inhibitor of the Epidermal Growth Factor Receptor Tyrosine Kinase, in Symptomatic Patients With Non–Small Cell Lung CancerA Randomized Trial. *JAMA* **290**, 2149–2158 (2003).

108. Psyrri, A. *et al.* Effect of Epidermal Growth Factor Receptor Expression Level on Survival in Patients with Epithelial Ovarian Cancer. *Clin. Cancer Res.* **11**, 8637 LP – 8643 (2005).

109. Patrick, G. N. *et al.* Conversion of p35 to p25 deregulates Cdk5 activity and promotes neurodegeneration. *Nature* **402**, 615–622 (1999).

110. Amit, I. *et al.* A module of negative feedback regulators defines growth factor signaling. *Nat. Genet.* **39**, 503–512 (2007).

111. Khan, I. & Steeg, P. S. Endocytosis: a pivotal pathway for regulating metastasis. *Br. J. Cancer* **124**, 66–75 (2021).

112. Mostov, K., Su, T. & ter Beest, M. Polarized epithelial membrane traffic: conservation and plasticity. *Nat. Cell Biol.* **5**, 287–293 (2003).

113. Winograd-Katz, S. E. & Levitzki, A. Cisplatin induces PKB/Akt activation and p38MAPK phosphorylation of the EGF receptor. *Oncogene* **25**, 7381–7390 (2006).

114. Ferguson, F. M. *et al.* Synthesis and structure activity relationships of a series of 4-amino-1H-pyrazoles as covalent inhibitors of CDK14. *Bioorg. Med. Chem. Lett.* **29**, 1985–1993 (2019).

115. Posadas, E. M. *et al.* A phase II and pharmacodynamic study of gefitinib in patients with refractory or recurrent epithelial ovarian cancer. *Cancer* **109**, 1323–1330 (2007).

116. Chelariu- Raicu, A. *et al.* Phase I/II study of weekly topotecan and gefitinib in patients with platinum-resistant ovarian, peritoneal, or fallopian tube cancer. *J. Clin. Oncol.* **38**, 6059 (2020).

7. Publications

1.p27kip1 expression and phosphorylation dictate Palbociclib sensitivity in KRAS-mutated Colorectal Cancer

Rampioni Vinciguerra GL, Dall'Acqua A, Segatto I, Mattevi MC, Russo F, Favero A, Cirombella R, Mungo, G, Viotto D, **Karimbayli J**, Pesce M, Vecchione A, Belletti B and Baldassarre G. Cell Death Dis. 2021 Oct 15;12(10):951. doi: 10.1038/s41419-021-04241-2.

8. Acknowledgements

For this fruitful journey I am sincerely grateful to specially my supervisor Dr.Gustavo Baldassare and my tutor Dr.Ilenia Pellarin, excellent scientists and wonderfully kind personalities, for their continuous and always available expertise/support not only in research, but also in daily life whenever I needed.

I also feel lucky to be surrounded by wonderful the whole CRO-OS2 team for having their kind support, expertise. Specifically, I thank Dr.Sara D'Andrea for her always available help throughout the PhD period.

I also thank my co-supervisor prof. Guidalberto Manfioletti for his support throughout my whole PhD spell.

I also express my thankfulness to my peers/friends Lorena, Alice..G, Albina, Lucrezia, Rob, Gionatan, Lorenzo for making small Aviano town lively with their kind friendship.

Overall, thanks to these people I happily feel Italy my second home.

I deliver my gratefulness to my dearest friend Dr.Ughur Aghamaliyev for his invaluable friendship and his support, since we met.

My gratefulness also extends to much beloved special teacher Lala, for her making black and white days colourful.

Finally, my utmost thanks belong to my family, my dad, Javanshir, my mom Gulnisa, and my brother Fuad, for their in-built support in my life.

With all due respect to my seniors, I dedicate this project to my dad, who is currently fighting against cancer. I wish this work would set a foundation that may one day help somebody to defeat cancer.